For Reference

NOT TO BE TAKEN FROM THIS ROOM

For Reference

NOT TO BE TAKEN FROM THIS ROOM

Ex LIBRIS
UNIVERSITATIS
ALBERTHAENSIS

QUAECUMQUE VERA

UNIVERSITY OF ALBERTA
LIBRARY

Regulations Regarding Theses and Dissertations

Typescript copies of theses and dissertations for Master's and Doctor's degrees deposited in the University of Alberta Library, as the official Copy of the Faculty of Graduate Studies, may be consulted in the Reference Reading Room only.

A second copy is on deposit in the Department under whose supervision the work was done. Some Departments are willing to loan their copy to libraries, through the inter-library loan service of the University of Alberta Library.

These theses and dissertations are to be used only with due regard to the rights of the author. Written permission of the author and of the Department must be obtained through the University of Alberta Library when extended passages are copied. When permission has been granted, acknowledgement must appear in the published work.

This thesis or dissertation has been used in accordance with the above regulations by the persons listed below. The borrowing library is obligated to secure the signature of each user.

Please sign below:

Date	Signature	Institution

THE UNIVERSITY OF ALBERTA

THE WEAK INTERACTION INDUCED PRESSURE DUE TO THE STEPWISE-DECELERATION OF A FLAT PLATE IN HYPERSONIC FLOW

BY

ROOP NARAYAN GUPTA B.E.(HONS.)

C

A THESIS

SUBMITTED TO THE FACULTY OF GRADUATE STUDIES

IN PARTIAL FULFILMENT OF THE REQUIREMENTS FOR THE DEGREE

OF MASTER OF SCIENCE

DEPARTMENT OF MECHANICAL ENGINEERING

EDMONTON, ALBERTA

APRIL, 1968

UNIVERSITY OF ALBERTA

FACULTY OF GRADUATE STUDIES

The undersigned certify that they have read, and recommend to the Faculty of Graduate Studies for acceptance, a thesis entitled "THE WEAK INTERACTION INDUCED PRESSURE DUE TO THE STEPWISE-DECELERATION OF A FLAT PLATE IN HYPERSONIC FLOW" submitted by ROOP NARAYAN GUPTA in partial fulfilment of the requirements for the degree of Master of Science.

ABSTRACT

A semi-infinite plate is exposed to the stepwise-decelerated hypersonic flow at zero angle of attack. The boundary layer reconfiguration gives rise to an induced pressure. To obtain this temporal pressure distribution, the transformed momentum and energy equations have been solved using the approach of Ref. [3] where the solutions are obtained in the range $0 \leq \tau \leq 1$. These solutions, with extension to the range $1 < \tau \leq 1.3$, are used to evaluate the displacement thickness for the unsteady boundary layer. The differentiated displacement thickness is finally used in the induced pressure expression involving the acoustic approximation. A family of curves is obtained, for the initial zero pressure gradient case, covering the range $0 \leq g_w \leq 1 + (\frac{\gamma-1}{2}) M_e^2$, $5 \leq M_e \leq 30$ and $0 \leq \tau \leq 1.3$. The shearing stress and heat transfer at the wall are obtained for the indicated range of g_w and M_e and $0 \leq \tau \leq 1.8$. The absolute magnitude of the transient contribution to the induced pressure distribution is found to be greater for the case of no heat transfer at the wall and $0 \leq g_w < 1$, and smaller for $g_w \geq 1$ as compared to the corresponding contribution for the case of stepwise-accelerated flow treated in Ref. [3]. Some attempts have also been made to improve the solution of the momentum equation by modifying the numerical method of Ref. [3].

ACKNOWLEDGEMENTS

The author wishes to extend his appreciation to Dr. C.M. Rodkiewicz for his guidance and supervision of this thesis.

Thanks are also extended to Miss H. Wozniuk for her excellent typing of the thesis and to the National Research Council for the funds under grant no. NRC A-4198, which were instrumental in the completion of the thesis.

TABLE OF CONTENTS

		Page
ABSTRACT		ii
ACKNOWLEDGEMENTS		iii
TABLE OF CONTENTS		iv
LIST OF FIGURES		vi
LIST OF SYMBOLS		ix
CHAPTER I	STATEMENT OF THE PROBLEM AND ASSOCIATED LITERATURE	
	1.1 The Unsteady Hypersonic Flow Problem	1
	1.2 Review of Previous Work	5
CHAPTER II	THE GOVERNING EQUATIONS	
	2.1 General Form of the Equations	12
	2.2 Dorodnitsyn-Howarth Transformation	13
	2.3 Similarity Forms	14
	2.4 Linearization of the Problem	18
	2.5 Associated Boundary and Time Conditions	20
CHAPTER III	SOLUTIONS TO THE GOVERNING EQUATIONS	
	3.1 Numerical Solution to the Momentum Equation	25
	3.2 Solution to the Energy Equation	28
	3.3 Shearing Stress at the Wall	29
	3.4 Heat Transfer at the Wall	30
CHAPTER IV	VISCOUS INTERACTIONS	
	4.1 The Displacement Thickness	31
	4.2 Steady State Boundary Layer Thickness	33
	4.3 Weak Interaction Induced Pressure	34
CHAPTER V	DISCUSSION AND CONCLUSIONS	
	5.1 Discussion of Results	39
	5.2 Concluding Remarks	44

		Page
BIBLIOGRAPHY		
APPENDIX 'A'	RECURRENCE RELATIONS INVOLVING THE 11-POINT MOLECULE	
	A.1 Formation of the Difference Equation	49
	A.2 Derivation of the Recurrence Relations	51
	A.3 Reasons for the Unstability	56
APPENDIX 'B'	GAUSS'S ELIMINATION METHOD	
	B.1 Formation of the Problem in a Tridiagonal System	58
	B.2 Gauss Elimination for a Tridiagonal System	61
APPENDIX 'C'	ITERATIVE FINITE DIFFERENCE METHOD INVOLVING THE 7-POINT MOLECULE	
	C.1 Formation of the Difference Equation	65
	C.2 Iterative Finite Difference Method	68
APPENDIX 'D'	ITERATIVE FINITE DIFFERENCE METHOD INVOLVING THE 11-POINT MOLECULE	71
APPENDIX 'E'	EFFECTS OF THE VARIATION OF GRID SIZE	74
APPENDIX 'F'	CURVES FOR CHAPTER III & IV	76

LIST OF FIGURES

Fig. No.		Page
1.1	Hypersonic Flow Over a Flat Plate	3
1.2	Stewartson's Impulsive Plate Problem	7
2.1	Velocity Profiles Due to the Stepwise Deceleration of Flow	19
2.2	Blasius Function $f(\eta)$ for the Initial and the Final Steady States	23
2.3	Blasius Function $f'(\eta)$ for the Initial and the Final Steady States	23
3.1	7-Point Molecule	26
3.2	11-Point Molecule	27
3.3	Stream Function Increment (Δf) Distribution Curve	77
3.4	Profiles of Stream Function Increment (Δf)	77
3.5	Distribution of the Derivatives of Δf (for τ=0.1) and Verification of the Satisfaction of the Differential Equation	78
3.6	Distribution of the Derivatives of Δf (for τ=0.7) and Verification of the Satisfaction of the Differential Equation	79
3.7	Distribution of the Derivatives of Δf (for τ=1.3) and Verification of the Satisfaction of the Differential Equation	79
3.8	Distribution of the Shearing Stress at the Wall as Function of τ	80
4.1	Boundary Layer Thickness Over a Flat Plate as Function of $\bar{\chi}$	81

Fig. No.		Page
4.2	Boundary Layer Thickness Over a Flat Plate as Function of M_e (For Zero Heat Transfer at the Wall)	81
4.3a	Transient Contribution to the Induced Pressure for the Case of No Heat Transfer at the Wall as Function of $\bar{\chi}$	82
4.3b	Transient Contribution to the Induced Pressure for the Case of No Heat Transfer at the Wall as Function of $\bar{\chi}$ (Stepwise Accelerated Flow)	82
4.3c	Transient Contribution to the Induced Pressure for the Case of No Heat Transfer at the Wall as Function of τ	83
4.4a	Transient Contribution to the Induced Pressure for the Case of $g_w = 0$ as Function of $\bar{\chi}$	
4.4b	Transient Contribution to the Induced Pressure for the Case of $g_w = 0$ as Function of $\bar{\chi}$ (Stepwise-Accelerated Flow)	84
4.4c	Transient Contribution to the Induced Pressure for the Case of $g_w = 0$ as Function of τ	
4.5a	Transient Contribution to the Induced Pressure for the Case of $g_w = 0.5$ as Function of $\bar{\chi}$	86
4.5b	Transient Contribution to the Induced Pressure for the Case of $g_w = 0.5$ as Function of $\bar{\chi}$ (Stepwise-Accelerated Flow)	86
4.5c	Transient Contribution to the Induced Pressure for the Case of $g_w = 0.5$ as Function τ	87
4.6a	Transient Contribution to the Induced Pressure for the Case of $g_w = 1.0$ as Function of $\bar{\chi}$	88
4.6b	Transient Contribution to the Induced Pressure for the Case of $g_w = 1.0$ as Function of $\bar{\chi}$ (Stepwise-Accelerated Flow	88
4.6c	Transient Contribution to the Induced Pressure for the Case of $g_w = 1.0$ as Function of τ	89

Fig. No.		Page
4.7	Transient Contribution to the Induced Pressure for the Case of $\bar{\chi}$ = 3.5, and M_e = 10	90
4.8	Transient Contribution to the Induced Pressure for the Case of $\bar{\chi}$ = 3.5, and M_e = 20	91

LIST OF SYMBOLS

a	velocity of sound
a	a function of g_w in equation (4.25)
a	coefficient in difference equations (A.9), (B.1), and (C.7)
A	a constant
A	coefficient in difference equation (D.1)
b	coefficient in difference equations (A.9), (B.1), and (C.7)
B	coefficient in difference equation (D.1)
C	a function of η and τ
C	= C(x) or a constant
C	coefficient in difference equation (D.1)
c_p	specific heat at constant pressure
d	coefficient in difference equations (A.9), (B.1) and (C.7)
D	coefficient in difference equation (D.1)
e	coefficient in difference equation (C.7)
e	a constant
E	coefficient in difference equation (D.1)
f	function related to the stream function by $f(\eta,\tau) = \psi\sqrt{\left[\frac{(m+1)}{2\nu_\infty CxU_e}\right]}$
F	coefficient in difference equation (D.1)
g	function related to enthalpy by $g(\eta,\tau) = h/G(x,t)$

G	dependent variable used in the energy equation
h	enthalpy
H	step size in the η-direction
I	integral appearing in the displacement thickness
J	integral appearing in the displacement thickness
k	thermal conductivity
m	a constant
m	an integer in numerical method
M	Mach Number
n	an integer in numerical method
N	value of n for which "e" condition prevails
p	thermodynamic pressure
Pr	Prandtl Number
q	heat transfer per unit time and per unit area
R	a function of η and τ
Re	Reynolds Number
S	$\equiv\Delta f$ (stream function increment), used in the computer programming
t	time
T	absolute temperature
T	step size in the τ-direction
U	stream velocity outside the boundary layer in x-direction
u	velocity component parallel to wall in boundary layer
v	velocity component normal to wall in boundary layer
x	cartesian co-ordinate parallel to wall
y	cartesian co-ordinate normal to wall

Y	modified co-ordinate in y-direction
α_1	as defined by equation (3.11)
α_2	as defined by equation (3.17)
β	a constant
γ	ratio of specific heats
δ^*	displacement thickness as defined by equation (1.1) or (4.3)
δ_ρ	as defined by equation (4.4)
Δ	displacement height (unsteady)
η	similarity independent variable associated with space
λ	as defined by equation (4.25)
μ	dynamic viscosity coefficient
ν	kinematic viscosity coefficient
ρ	density
τ	shear stress
τ	similarity independent variable associated with time and space
$\overline{\chi}$	hypersonic similarity variable as defined by expression (4.19)
ψ	stream function

Subscripts

w	evaluation at wall (y=0)
e	evaluation in free stream ($y=y_e$)
Ref	reference
∞	flow ahead of the shockwave
1	initial steady state
2	final steady state

CHAPTER I

STATEMENT OF THE PROBLEM AND ASSOCIATED LITERATURE

1.1 The Unsteady Hypersonic Flow Problem

The theory of unsteady compressible boundary layers has not been extensively studied in the past. One of the reasons for this is that, in many engineering problems, boundary layer growth occurs in so short a time that it is often sufficient to assume the steady state although the speed changes with space and time. There are cases, however, where a more detailed investigation is desirable. These cases include, for instance, oscillating wings, blades rotating in non-uniform air streams, unsteady nozzle flow and aircrafts and missiles in unsteady flight. The maneuverability and control of aircrafts and missiles is completely dependent upon the forces acting on the components of these aerodynamic vehicles. In evaluating these forces viscous interactions must be considered. The research on the blunt-leading-edge and the sharp-leading-edge bodies is the best source of information on viscous interaction phenomenon.

The problem to be considered herein is the interaction between the viscous and inviscid effects. The initial zero angle of attack, high Mach Number flow is stepwise-decelerated by a small amount in the direction of the initial flow. In order to obtain the interaction induced pressure, the development of the velocity and enthalpy boundary layers will be considered first. From this growth of the boundary layers, equations will be

derived which will account for the effects of the interaction between the viscous and inviscid flow upon surface skin friction, heat transfer and the normal forces on the plate.

Within a hypersonic boundary layer, the temperature is expected to be high, which means that the density will be low and the equation

$$\delta^* = \int_0^\infty \left(1 - \frac{\rho u}{\rho_e U_e}\right) dy \qquad (1.1)$$

serves to indicate that the displacement thickness will be large. Ordinarily, this would be of no particular consequence except close to the leading edge of a sharp-nosed object. Near the sharp leading edge where the displacement thickness is increasing from zero, the turning of the flow external to the boundary layer causes an initial compression accompanied by a shock wave. This compression with the following flow expansion, in turn affects the build-up of the boundary layer, and thus we have a problem of interaction between the external inviscid flow and the boundary layer.

In the hot gas layer near the surface it is certainly not at all clear at first whether the usual Prandtl Boundary Layer Equations are applicable for hypersonic flow. However, Shen [1] has shown that when $(\delta/x)^2 \ll 1$, the higher order viscous and heat conduction terms $[(\mu u_x)_x, (kT_x)_x]$ in the x-momentum and energy equations are small compared to the terms $(\mu u_y)_y$ and $(kT_y)_y$. In addition the static pressure ratio across the boundary layer is negligible.

The problem, then, is to determine the solutions for a classical

Prandtl boundary layer subjected to an "external pressure gradient" which is not known in advance, but which depends on the growth of the boundary layer itself.

Lees and Probstein [2] have divided the total flow region into two main regions: I, a "leading edge" region; II, a region of "no-slip" as shown in Fig. 1.1

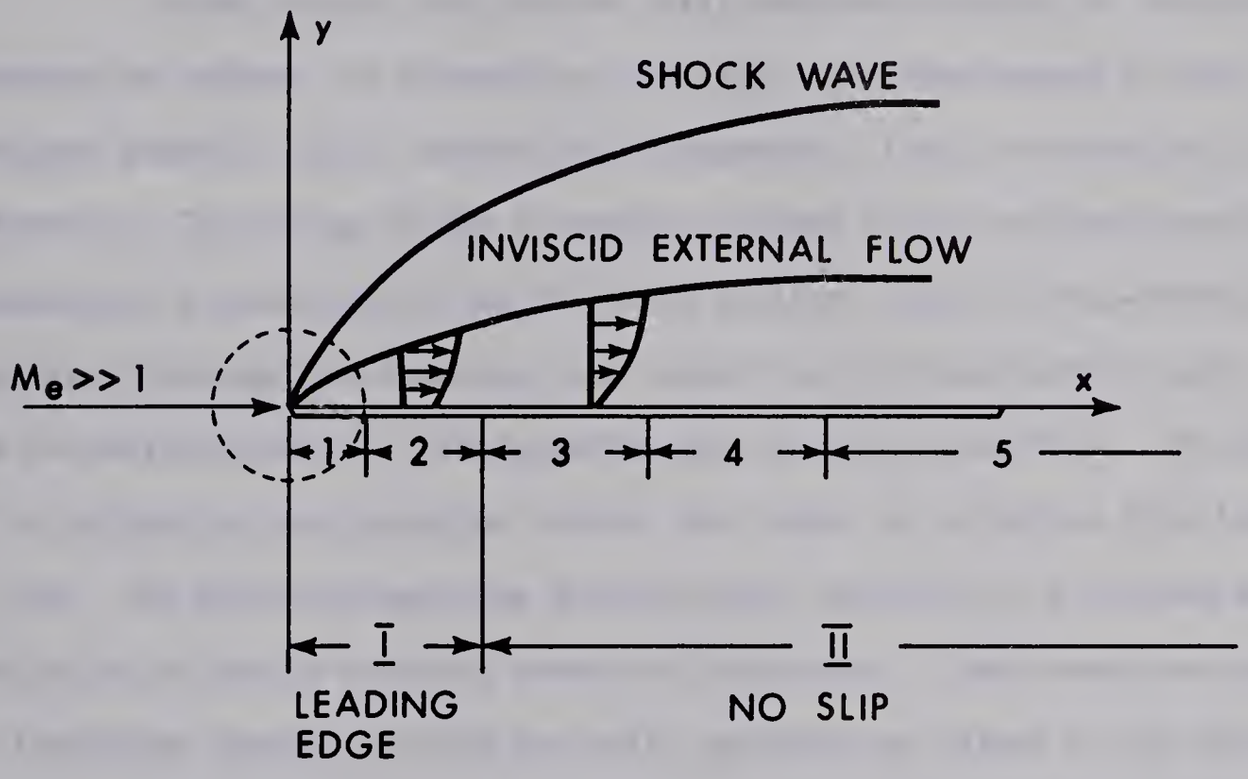

Fig. 1.1
Hypersonic Flow Over a Flat Plate

Breaking the leading edge region into two sub-regions indicated by 1 and 2 in Fig. 1.1, they point out a relatively small domain "1" around the leading edge which is of the order of 20 mean free paths in breadth and domain "2", the slip flow region.

In region II, as pointed out by Lees and Probstein, slip and temperature jump at the surface are negligible, and the continuum-flow-

concepts apply throughout. The no-slip region is further subdivided into three domains: (3) strong interaction region; (4) transition region; (5) weak interaction region. Based upon the observations of the authors of Ref. [2], the strong interaction region should be important only for flight Mach Numbers greater than about 15.

In the present analysis we shall confine ourselves to the weak interaction regime. As pointed out previously the development of the unsteady boundary layer, especially in hypersonic flow, has received little attention. The review of the literature related to the problem under consideration is presented in the following section. Next the two-dimensional nonsteady compressible boundary layer equations are transformed, using the Dorodnitsyn-Howarth transformation and the stream function. The use of a similarity transformation reduces the number of variables from three to two. The resulting momentum and the energy equations are coupled and can not be solved by ordinary numerical techniques. These equations may be linearized keeping in view the small perturbation nature of the problem. The linearization technique used here is similar to that of Ref. [3]. For zero pressure gradient case the linearized momentum and the energy equations become uncoupled but still the nature of the momentum equation does not permit a closed form solution. Therefore the numerical method for its solution was adopted. Ordinary type of numerical methods did not succeed. A summary of these methods has been included in the appendices. The iterative finite difference method of Appendix 'C' was found to give the desired solution of the momentum equation. However, the method was too costly computer time-wise. Instead the numerical method developed in

Ref. [3] was used with some changes in the computational technique. With these changes the solution of the momentum equation was available for $0 \leq \tau \leq 1.3$. The solution of the energy equation was obtained for the adiabatic wall as well as for finite heat transfer at the wall from the existing literature [3].

The shearing stress at the wall was directly obtained from the solution of the momentum equation. The differentiated displacement thickness was used to obtain the normal pressure distribution involving the acoustic approximation. The variation of the steady state boundary layer thickness was also obtained for zero and non-zero heat transfer at the wall. The relevant results have been discussed in the last chapter.

1.2 Review of Previous Work

Blasius was the first (see paragraph 65, Ref. [21]) to investigate the unsteady laminar boundary layer flow over various bodies starting from rest. Several other investigators also analysed the unsteady boundary layer flow for special cases. F.K. Moore [22] included in his treatment the unsteady boundary layer flow for longer times elapsed since starting and for higher speeds. He considered the case of compressible laminar flow over a semi-finite flat plate in rectilinear accelerated flight through still air. In his analysis he found that a group of parameters

$$\frac{xU_e'}{U_e^2} ; \frac{x^2U_e''}{U_e^3} ; \ldots \frac{x^nU_e^{(n)}}{U_e^{n+1}} ; \ldots \qquad (1.2)$$

can be formed incorporating the coordinate along the surface and the free stream velocity and its derivatives. For uniform acceleration ($U_e = AT$), the quantities (1.2) reduce to a single paramater $\zeta = x/AT^2$ $(=\frac{1}{\tau})$. For $\zeta >> 1$, the effect of the leading edge has not been felt at the station x and the classical "starting-from-rest" solution applies. If $\zeta << 1$, the growth of the boundary layer with x must be considered and Ref. [22] points out that the flow may be regarded as nearly quasi-steady; that is, at any instant the motion is nearly that which would be obtained in steady flow at the conditions prevailing at that instant. Moore considered an insulated flat plate problem. Ostrach's [6] extension includes the heat transfer over an isothermal surface.

K. Stewartson [7] studied the fluid motion induced by the uniform motion of a semi-infinite flat plate in its own plane. Using the stream function ψ defined by

$$\psi = U_\infty (\nu t)^{1/2} \phi(\zeta, \tau) \qquad (1.3)$$

with

$$\tau = \frac{U_\infty t}{x} , \quad \zeta = \frac{y}{(\nu t)^{1/2}}$$

Stewartson expands ϕ in a power series in τ with coefficients that are functions of ζ. This series has as the leading term the error function solution of the Rayleigh Problem in the sense of $\frac{\partial \phi}{\partial \zeta} = \text{erf}\, \frac{\zeta}{2}$, $\tau \to 0$, and all subsequent terms are identically zero. He then indicates that an essential singularity is likely to exist at $\tau = 1$, $\zeta \to \infty$. However,

no such singularity may be expected for $0 \leq \tau < 1$. He also points out that the Rayleigh solution valid for $\tau < 1$, may be joined nonanalytically at $\tau = 1$ to some x-dependent solution valid for $\tau > 1$. Stewartson further explains why the x-dependence can not enter via a power series to describe the transition from a function of (y,t) in $U_\infty t < x$ to a function of (y,t,x) in $U_\infty t > x$. In order to explain the disappearance of t-dependence as $\tau \to \infty$ where ϕ must approach the Blasius function, he mentions that the terms depending on t may be exponentially small.

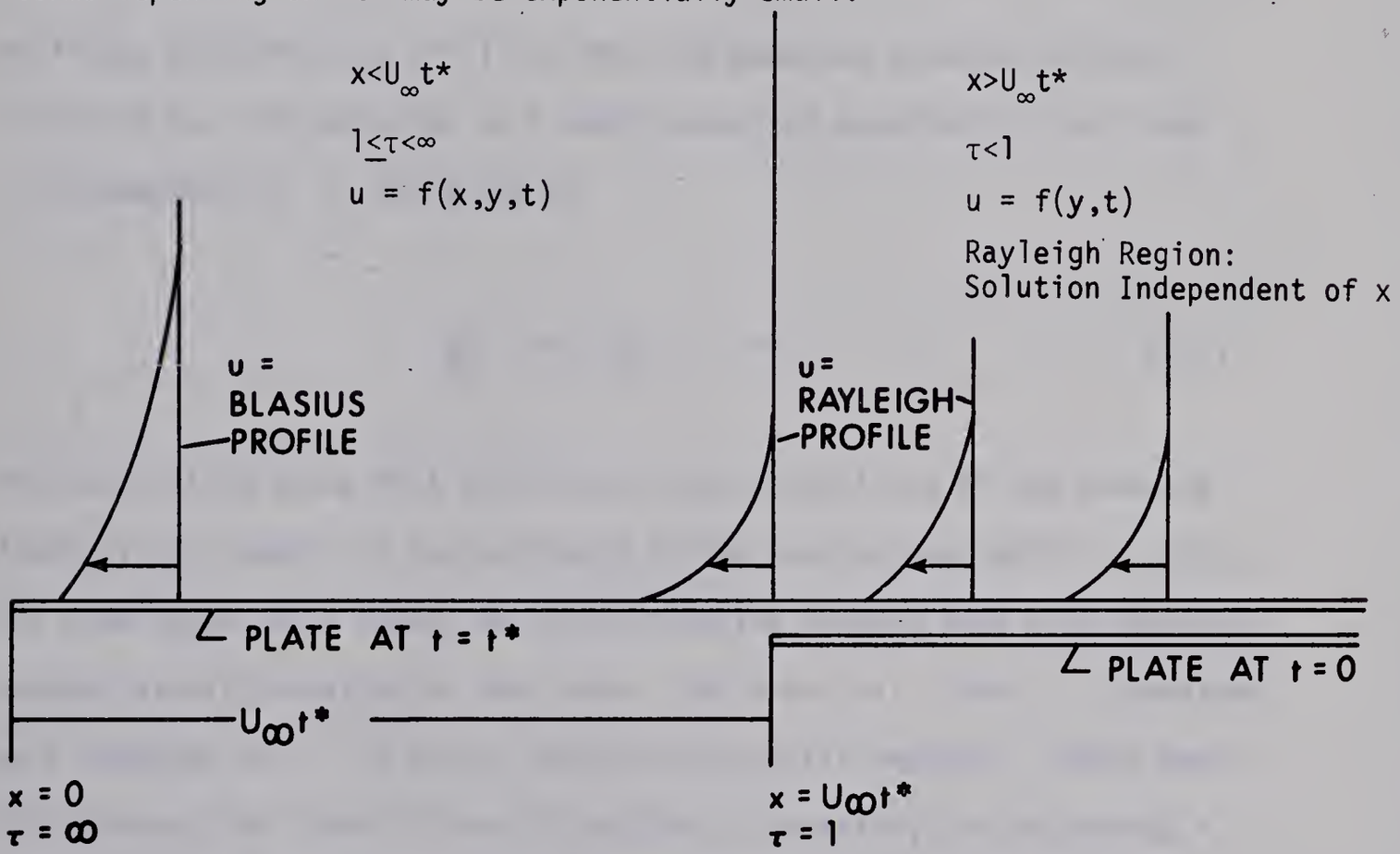

Fig. 1.2
Stewartson's Impulsive Plate Problem

In his later publication [8] Stewartson shows that the asymptotic behavior for large τ (Blasius) is not relevant to the solution in $\tau<1$ (Rayleigh). Considering $\frac{\partial\phi}{\partial\zeta}$ as the dependent variable and taking the coefficient of the mixed derivative as

$$k = \tau - \tau^2 \frac{\partial\phi}{\partial\zeta}$$

he finds, with the help of (1.3), that the momentum equation in the x-direction has the character of a heat conduction equation in $\tau<1$ and ϕ is independent of τ and given by

$$\frac{\partial\phi}{\partial\zeta} = \text{erf}\ (\tfrac{\zeta}{2}) \quad ; \quad \tau<1 \,. \tag{1.4}$$

Physically this means that the fluid at any point (x,y) of the boundary layer is not "aware" of the existence of the leading edge until $t = x/U_\infty$, the time taken for a signal to travel from the leading edge with the mainstream velocity relative to the plate. But when $\tau>1$, then k, regarded as a function of ζ is partly positive and partly negative. Hence small disturbances now travel in both directions (increasing and decreasing τ) so that the solution must depend on conditions at $\tau=\infty$ and at $\tau= 1$. Again we may say that the fluid at (x,y) when $t>x/U_\infty$ is "aware" of the leading edge and its previous (downstream) history.

The work of Lam and Crocco [9] gives details of the growth of boundary layer induced by a shock travelling down a semi-infinite flat

plate. At $t=0$ the shock is at the leading edge of the plate, $x=0$. For the special case of a very weak shock the problem becomes identical to Stewartson's impulse plate problem. Using the Prandtl boundary layer equations under the Crocco transformation they have given sufficient conditions for unique solution to the governing equations for the case $\rho\mu$ = const. The treatment of the equations is consistent with the physics of the problem corresponding to situations in a shock tube. The boundary layer is divided into two parts: I, a region where the old solution of Mirels [10] is valid ($\tau<1$); II, the region, $\tau>1$, where the leading edge effects and the effect of the shock solution downstream both must be considered. τ is, again, here, taken as $U_e t/x$.

Cheng [11], while considering the problem of a sharp-edged flat plate started from rest in an incompressible fluid, expands the stream function in powers of the quantity.

$$\xi = \frac{x}{U_e t} \left(= \frac{1}{\tau}\right)$$

he obtains an approximate solution downstream of the leading edge and points out that the solution can be continued as far downstream as one wishes. The formal difficulty of the appearance of "an essential singularity" at $\xi=1$ and $\eta=\infty$, encountered by him and Stewartson in the method of perturbing the Rayleigh type solution, disappears. Cheng in his later publication along with Elliot [13] included in his treatment an arbitrary plate velocity and the effects of compressibility.

Schuh's [23] approach is based on the use of approximate momentum integral method (Pohlhausen-Method in the wider sense). Using the parameter

$$\tau = \frac{tu_0}{c}$$

he obtains the growth of the boundary layer over a circular cylinder and also the development of the boundary layer and the frictional drag over a flat plate of finite length for the case of impulsive start from rest and for the case of steady acceleration. In the expression for τ, u_0 is the constant reference speed and c is the characteristic length. Schuh noticed that there is a discontinuity in slope of the skin friction distribution for a flat plate in the range $1<\tau<\infty$.

On examination of the literature pertinent to the unsteady compressible boundary layers, it becomes evident that τ should be one of the parameters to be used in such analysis. It is indicated in reference [3] that

$$\eta = \sqrt{\left[\frac{(m+1)\ U_e}{2\nu_{ref}\ cx}\right]}\ Y, \quad \text{and} \quad \tau = \frac{U_e t}{x}$$

are the proper variables to transform the non-steady boundary layer equations to similarity forms.

Based on the "Piston Theory" of Lighthill [14], which was supplemented by Landhal [15] and Miles [16], it has been pointed out in Ref.

[3] that

$$\frac{\partial U_e}{\partial t} = \frac{\partial h_e}{\partial t} = 0 . \qquad (1.5)$$

Giving details of the above expressions it has been mentioned that one obtains an equivalent of the Ackeret pressure distribution instantaneously on the plate at large Mach Numbers.

CHAPTER II

THE GOVERNING EQUATIONS

2.1 General Form of the Equations

The Prandtl boundary layer equations in the unsteady form are taken as the equations governing the flow in a compressible, unsteady, laminar, two-dimensional boundary layer. They are [8, 17]:

$$\rho \left(\frac{\partial u}{\partial t} + u \frac{\partial u}{\partial x} + v \frac{\partial u}{\partial y}\right) = - \frac{\partial p}{\partial x} + \frac{\partial}{\partial y} \left(\mu \frac{\partial u}{\partial y}\right) \tag{2.1}$$

$$\frac{\partial p}{\partial y} = 0 \tag{2.2}$$

$$\rho \left(\frac{\partial h}{\partial t} + u \frac{\partial h}{\partial x} + v \frac{\partial h}{\partial y}\right) = \frac{\partial p}{\partial t} + u \frac{\partial p}{\partial x} + \frac{\partial}{\partial y} \left(\frac{\mu}{Pr} \frac{\partial h}{\partial y}\right) + \mu \left(\frac{\partial u}{\partial y}\right)^2 \tag{2.3}$$

$$\frac{\partial \rho}{\partial t} + \frac{\partial}{\partial x} (\rho u) + \frac{\partial}{\partial y} (\rho v) = 0 \tag{2.4}$$

with the boundary conditions

$$\begin{aligned} &\text{when } y = 0, && u = v = 0 \\ & && h = h_w(x,t) \\ &\text{when } y = y_e && u = U_e(x,t) \\ & && h = h_e(x,t) \end{aligned} \tag{2.5}$$

The pressure in the boundary layer, being independent of y, may be given by its value of $y=y_e$ according to the inviscid solution:

$$\rho_e \left(\frac{\partial U_e}{\partial t} + U_e \frac{\partial U_e}{\partial x}\right) = - \frac{\partial p}{\partial x} \tag{2.6}$$

where U_e denotes the prescribed potential motion.

2.2 Dorodnitsyn-Howarth Transformation

Using the Dorodnitsyn-Howarth transformation [8]

$$Y = \int_0^y \frac{\rho}{\rho_\infty} dy \tag{2.7}$$

and defining the stream function as

$$\frac{\partial \psi}{\partial y} = \frac{\rho}{\rho_\infty} u \tag{2.8}$$

the boundary layer equations become

$$\frac{\partial^2 \psi}{\partial Y \partial t} + \frac{\partial \psi}{\partial Y} \frac{\partial^2 \psi}{\partial x \partial Y} - \frac{\partial \psi}{\partial x} \frac{\partial^2 \psi}{\partial Y^2} = \frac{\rho_e}{\rho} U_e \frac{\partial U_e}{\partial x} + c\nu_\infty \frac{\partial^3 \psi}{\partial Y^3} \tag{2.9}$$

$$\frac{\partial h}{\partial t} + \frac{\partial \psi}{\partial Y} \frac{\partial h}{\partial x} - \frac{\partial \psi}{\partial x} \frac{\partial h}{\partial Y} = - \frac{\rho_e}{\rho} \frac{\partial \psi}{\partial Y} U_e \frac{\partial U_e}{\partial x} + \nu_\infty \frac{C}{Pr} \frac{\partial^2 h}{\partial Y^2} + \nu_\infty C \left(\frac{\partial^2 \psi}{\partial Y^2}\right)^2 \tag{2.10}$$

where

$$u = \frac{\partial \psi}{\partial Y} \tag{2.11}$$

$$v = -\frac{\rho_\infty}{\rho}\left(\frac{\partial \psi}{\partial x} + \frac{\partial Y}{\partial t}\right) \tag{2.12}$$

It has been assumed that

$$C = C(x) = \frac{\mu\rho}{\mu_\infty \rho_\infty} \tag{2.13}$$

and that Pr and C_p are constant. The product $\mu\rho$ is evaluated at some point within the boundary layer so that it is independent of Y.

2.3 Similarity Forms

The following forms of the similarity variables [3] may be used in order to reduce the independent variables from three to two.

$$\eta = \sqrt{\left[\frac{(m+1)\, U_e}{2\nu_\infty\, cx}\right]}\, Y \tag{2.14}$$

$$\psi = \sqrt{\left[\frac{2\nu_\infty cx\, U_e}{(m+1)}\right]}\, f(\eta,\tau) \tag{2.15}$$

where

$$\tau = \frac{U_e t}{x} \tag{2.16}$$

and

$$U_e = U_e(x) \tag{2.17}$$

In addition, let

$$h = g(\eta,\tau)\ G(x,t) \tag{2.18}$$

On substituting (2.14) and (2.15) into the differential equations (2.9) and (2.10), one obtains

$$\dot{f}'\frac{U_e}{x} + f'^2\frac{\partial U_e}{\partial x} - U_e f'\dot{f}'\frac{\tau}{x} + f'\dot{f}'\tau\frac{\partial U_e}{\partial x} - \frac{1}{2x}ff''U_e + \dot{f}U_e f''\frac{\tau}{x}$$

$$- \dot{f}f''\tau\frac{\partial U_e}{\partial x} - \frac{1}{2}ff''\frac{\partial U_e}{\partial x} - \frac{h}{h_e}\frac{\partial U_e}{\partial x} - c\nu_\infty A^2\frac{U_e}{x}f''' = 0 \tag{2.19}$$

and

$$\dot{g}G\frac{U_e}{x} + g\frac{\partial G}{\partial t} - \tau G\dot{g}\frac{U_e}{x}f' + \tau m\frac{U_e}{x}G\dot{g}f' + g\frac{\partial G}{\partial x}U_e f'$$

$$- \frac{1}{2}\frac{U_e}{x}Gfg' - \frac{1}{2}m\frac{U_e}{x}fg' + \tau\frac{U_e}{x}\dot{f}Gg' - \tau\dot{f}Gg'm\frac{U_e}{x}$$

$$= -\frac{\rho_e}{\rho}U_e^2 f'm\frac{U_e}{x} + \frac{(m+1)}{2Pr}\frac{U_e}{x}Gg'' + \frac{(m+1)}{2}\frac{U_e^3}{x}f''^2 \tag{2.20}$$

where

$$A^2 = \frac{m+1}{2c\nu_\infty}$$

$$\dot{f} = \frac{\partial f}{\partial \tau}$$

$$f' = \frac{\partial f}{\partial \eta}$$

$$\dot{g} = \frac{\partial g}{\partial \tau}$$

and

$$g' = \frac{\partial g}{\partial \eta}$$

Let

$$U_e = ex^m \tag{2.21}$$

$$\beta = \frac{2m}{m+1} \tag{2.22}$$

and

$$G(x,t) = G(x) = h_e(x) \tag{2.23}$$

Using the energy equation for the free stream and expression (2.6), one obtains

$$\rho_e \frac{\partial h_e}{\partial x} = \frac{\partial p}{\partial x} = - \rho_e U_e \frac{\partial U_e}{\partial x}$$

and employing the power law distribution of expression (2.21), one may write

$$\frac{\partial h_e}{\partial x} = - m \frac{U_e^2}{x} \tag{2.24}$$

Substituting (2.22) through (2.24) into (2.19) and (2.20) one obtains, under the assumption of perfect gas, the equations given by Rodkiewicz [3], namely,

$$(2-\beta)\dot{f}' + 2(1-\beta)\tau(\dot{f}f'' - \dot{f}'f') - f''' - ff'' - \beta(g-f'^2) = 0 \tag{2.25}$$

$$\Pr(2-\beta)\left[1 - \frac{2(1-\beta)}{(2-\beta)}\tau f'\right]\dot{g} - g'' - \Pr[f - 2(1-\beta)\tau\dot{f}]\, g'$$

$$- \Pr(\gamma-1)\, M_e^2\, f''^2 = 0 \tag{2.26}$$

where

$$\frac{U_e^2}{h_e} = (\gamma-1)\, M_e^2$$

For the case of weak interactions (zero pressure gradient) equations (2.25) and (2.26) reduce to

$$2\dot{f}' + 2\tau(\dot{f}f'' - \dot{f}'f') - f''' - ff'' = 0 \tag{2.27}$$

$$2\Pr\,(1-\tau f')\,\dot{g} - g'' - \Pr(f-2\tau\dot{f})g' - \Pr(\gamma-1)\, M_e^2\, f''^2 = 0 \tag{2.28}$$

2.4 Linearization of the Problem

The flow pattern immediately following the start of an impulsive motion in a viscous fluid is necessarily the same as would occur in an inviscid fluid, except for the presence of (infinitely thin) vortex sheets along all solid boundaries. This follows from the fact that, in the case of a suddenly "created" velocity, the dominant terms in the Navier-Stokes equations are

$$\frac{\partial u}{\partial t} = - \frac{1}{\rho} \text{grad } p \qquad (2.29)$$

so that curl u = 0, i.e., a potential flow pattern would be found except near solid boundaries where the no slip condition causes the initial vortex sheet.

An interesting generalization of this result was pointed out by Sears [18], who considered an impulsive change superimposed on an already established flow pattern. He showed that the initial motion following any impulsive change of the boundary conditions consists of the superposition of the velocity pattern existing just before the change and the inviscid flow velocity pattern due to the impulsive boundary values (together with the corresponding infinitely thin wall vortex sheet). This is the result of equation (2.29) which dominates the pattern at the moment of change. The terms of this equations are all linear.

This would mean that the velocity pattern following the step-deceleration of a flat plate moving in Hypersonic viscous flow may be re-

presented as:

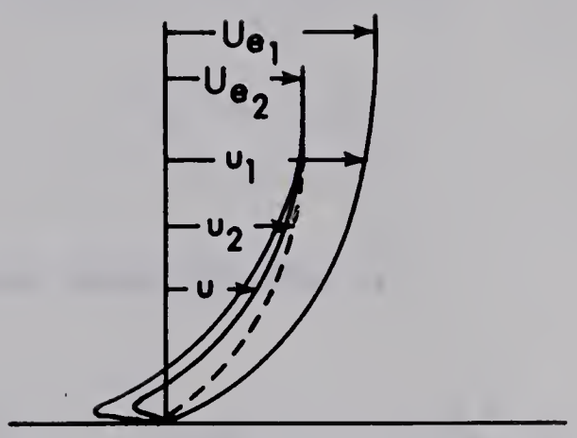

Fig. 2.1
Velocity Profiles

The dotted line indicates the final steady state.

Let us assume that

$$f(\eta,\tau) = f_2(\eta) - \Delta f(\eta,\tau) \tag{2.30}$$

where $f_2(\eta)$ satisfies the final steady state equations existing in the literature [13,14].

This type of linearization technique was used by Rodkiewicz [3] for a step-accelerated flat plate in Hypersonic flow.

Substitution of equation (2.30) into equation (2.27) results in

$$2(\dot{\Delta f})' + 2\tau[f_2''(\dot{\Delta f}) - f_2'(\dot{\Delta f})'] - (\Delta f)'''$$

$$- f_2(\Delta f)'' - f_2''(\Delta f) = 0 \tag{2.31}$$

where the second order terms in Δf have been dropped and the following

steady state momentum equation has been used

$$f_2''' + f_2 f_2'' = 0 \tag{2.32}$$

Also, the steady state energy equation is

$$g_2'' + Pr\, f_2\, g_2' + Pr(\gamma-1)\, M_e^2\, f_2''^2 = 0 \tag{2.33}$$

2.5 Associated Boundary and Time Conditions

When $y = 0$, $Y = 0$, $\eta = 0$, $u = 0$, $f'(0,\tau) = 0$, $f_2'(0) = 0$

and

$$(\Delta f)'(0,\tau) = 0 \tag{2.34}$$

when $y = 0$, $Y = 0$, $\eta = 0$, $\psi = 0$, $f(0,\tau) = 0$, $f_2(0) = 0$ and

$$\Delta f(0,\tau) = 0 \tag{2.35}$$

when $y = y_e$, $Y = Y_e$, $\eta = \eta_e$, $u = U_{e2}$, $f'(\eta_e,\tau) = 1$, $f_2'(\eta_e) = 1$ and

$$(\Delta f)'(\eta_e,\tau) = 0 \tag{2.36}$$

when $t = 0$, $\tau = 0$, $u = u_1 - (U_{e1} - U_{e2})$,

$$f'(\eta>0,0) = f_1' \frac{U_{e1}}{U_{e2}} - \left(\frac{U_{e1}}{U_{e2}} - 1\right) \text{ and}$$

$$(\Delta f)'(\eta>0,0) = - f_1' \frac{U_{e1}}{U_{e2}} + \left(\frac{U_{e1}}{U_{e2}} - 1\right) + f_2'(\eta) \qquad (2.37a)$$

This may be integrated to give

$$\Delta f(\eta>0,0) = - \sqrt{\left[\frac{U_{e1}}{U_{e2}}\right]}\, f_2\left(\sqrt{\left[\frac{U_{e1}}{U_{e2}}\right]}\,\eta\right) + \left(\frac{U_{e1}}{U_{e2}} - 1\right)\eta + f_2(\eta) \qquad (2.37b)$$

when $y = 0$, $Y = 0$, $\eta = 0$, $h = h_w$ and

$$g(0,\tau) = \frac{h_w}{h_{e2}} \qquad (2.38)$$

and for the case of an insulated plate

$$g'(0,\tau) = 0 \qquad (2.39)$$

when $y = y_e$, $Y = Y_e$, $\eta = \eta_e$, $h = h_{e2}$ and

$$g(y_e,\tau) = 1 \qquad (2.40)$$

when $t = 0$, $\tau = 0$, $h = h_1$ and

$$g(\eta,0) = \frac{h_1}{h_{e2}} \qquad (2.41)$$

At this stage it would be useful to note the relation between the quantities belonging to initial and final steady state conditions.

From the relation (2.14), one may write

$$\eta_1 = \sqrt{\left[\frac{m+1}{2\nu_\infty x}\right]}\, Y \sqrt{U_{e1}} \tag{2.42a}$$

$$\eta_2 = \sqrt{\left[\frac{m+1}{2\nu_\infty x}\right]}\, Y \sqrt{U_{e2}} \tag{2.42b}$$

From above, we obtain

$$\eta_2 = \eta_1 \sqrt{\frac{U_{e2}}{U_{e1}}} \quad \text{and} \quad d\eta_2 = \sqrt{\left[\frac{U_{e2}}{U_{e1}}\right]}\, d\eta_1 \tag{2.43}$$

If f_1 and f_2 satisfy equation (2.32) with the boundary conditions:

when $$\eta_1 = 0,\ f_1 = 0,\ f_1' = 0$$

$$\text{when} \quad \eta_1 = \eta_e,\ f_1' = 1 \tag{2.44}$$

when $$\eta_2 = 0,\ f_2 = 0,\ f_2' = 0$$

$$\text{when} \quad \eta_2 = \eta_e,\ f_2' = 1 \tag{2.45}$$

The two solutions must be the same and accordingly $f_1(\eta_1)$ and $f_2(\eta_2)$

may be related by the relation

$$f_1(\eta_1) = f_2(\sqrt{[\frac{U_{e2}}{U_{e1}}]}\eta_1) \tag{2.46}$$

If

$$\frac{U_{e1} - U_{e2}}{U_{e2}} = 0.01 \tag{2.47}$$

Then,

$$f_1(\eta_1) = f_2(0.995\eta_1) \tag{2.48}$$

This may be represented diagrammatically as:

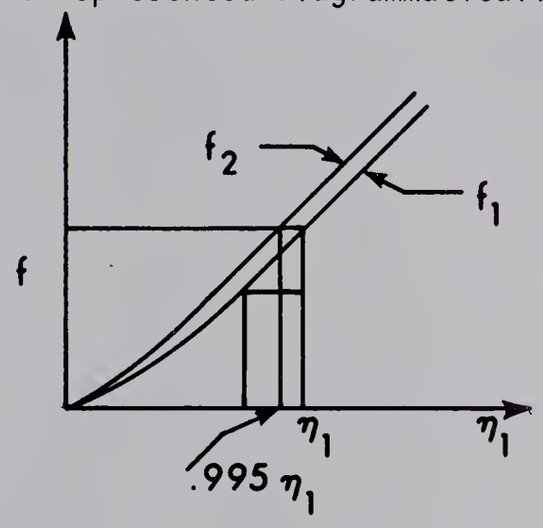

Fig. 2.2
Blasius Function f(η)

Similarly the velocity profile may be represented as:

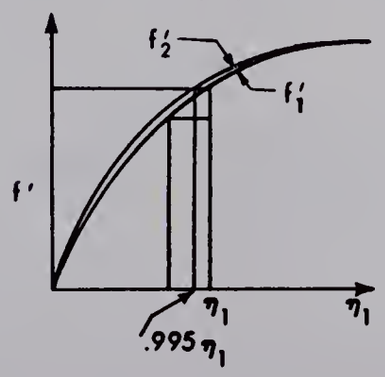

Fig. 2.3
Blasius Function f'(η)

From the figure one can easily see that

$$f_1'(n_1) = f_2'(n_2) = f_2'(0.995n_1) \tag{2.49}$$

CHAPTER III

SOLUTIONS TO THE GOVERNING EQUATIONS

3.1 Numerical Solution to the Momentum Equation

The solution to equation (2.31) with the time dependent boundary conditions (2.34) through (2.37) for the case of a stepwise-decelerated flat plate in viscous hypersonic flow is presented. In reference [3], where the case of a stepwise-accelerated flat plate has been considered, a numerical solution to equation (2.31) with the appropriate boundary conditions is discussed in detail. The difference in the two problems (of stepwise-accelerated and stepwise decelerated flat plate) arises from the boundary condition (2.37). The author of reference [3] has suggested the recurrance relation

$$S_{m,n} = R_{m,n}\, S_{m,n+1} + C_{m,n} \tag{3.1}$$

where

$$R_{m,n} = \frac{-a_{m,n}}{(b_{m,n} + c_{m,n}\, R_{m,n-1} + d_{m,n}\, R_{m,n-1}\, R_{m,n-2})} \tag{3.2}$$

and

$$C_{m,n} = \frac{e_{m,n} - (c_{m,n}\, C_{m,n-1} + d_{m,n}\, R_{m,n-2}\, C_{m,n-1} + d_{m,n}\, C_{m,n-2})}{(b_{m,n} + c_{m,n}\, R_{m,n-1} + d_{m,n}\, R_{m,n-1}\, R_{m,n-2})} \tag{3.3}$$

and where

$$R_{m,1} = C_{m,1} = C_{m,2} = 0,\ R_{m,2} = 0.25 \tag{3.4}$$

from the boundary conditions (2.34) and (2.35).

$a_{m,n}$, $b_{m,n}$, $c_{m,n}$, $d_{m,n}$ and $e_{m,n}$ are defined in Appendix 'C'.

For $n = N$, where the "e" condition prevails, the following relation has been suggested in view of the boundary condition (2.36).

$$S_{m,N} = \frac{C_{m,N-1} - \dfrac{C_{m,N-2}}{4-R_{m,N-2}}}{\dfrac{3}{4-R_{m,N-2}} - Rm,N-1} \qquad (3.5)$$

The computations are based on the following shape of the molecule:

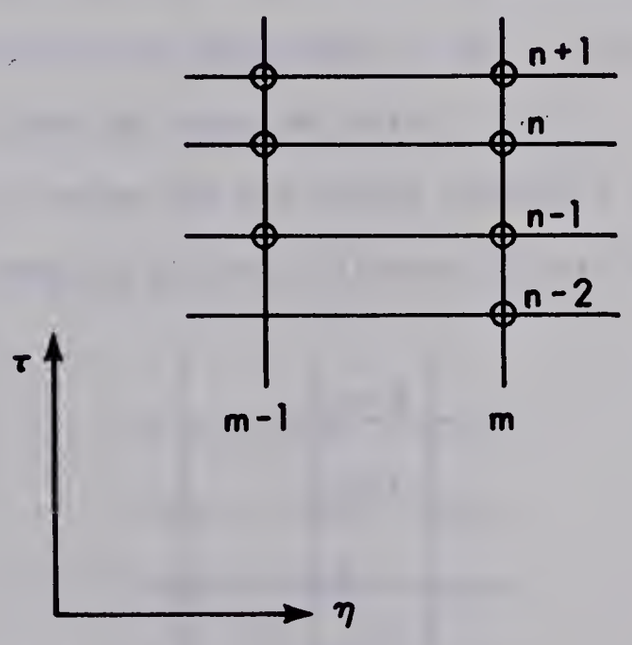

Fig. 3.1
7-Point Molecule

However, the numerical method did not produce consistent stream function increment (Δf) distribution for $\tau>1$. Some jumps were noted in the value Δf . A search was made by the present writer to find out the

"blow-up" causes. It was found that the term

$$\frac{3}{4-R_{m,N-2}} - R_{m,N-1} \qquad (3.6)$$

in expression (3.5) goes through zero as τ gets greater than one.

An iterative finite difference method was tried to get rid of the previously mentioned difficulty for $\tau>1$. The method did succeed in giving values upto $\tau = 1.2$. However, the numerical method was too costly computer time-wise and, therefore, it was given up finally. A summary of this method is included in the Appendix 'C'.

It was decided to use the numerical method of Ref. [3] with some improvement in the computational technique. In order to reduce the "Round-off" errors, double precision was used in the computations. With this change, Δf^* distribution was obtainable up to $\tau = 1.3$ and the shear stress at the wall could be computed up to $\tau = 1.8$.

In place of using the previously indicated 7-point molecule, some attempts were made to use the following 11-point molecule:

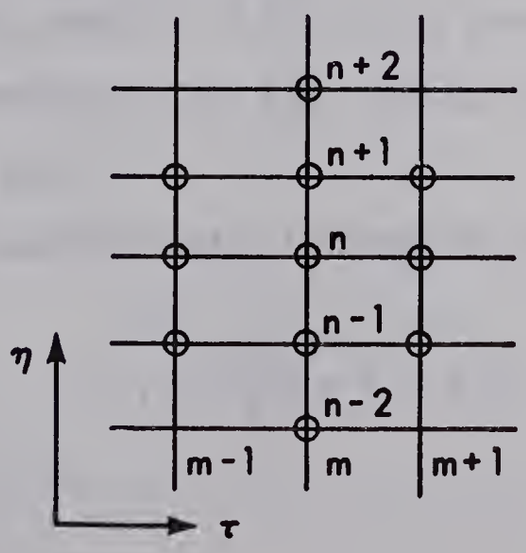

*See Appendix 'F' for the curves of Chapter III

This molecule is the result of applying the commonly used expressions for central derivatives. The third order derivative in η-direction is based now on points (m,n+2), (m,n+1), (m,n-1) and (m,n-2) instead of (m,n+1), (m,n), (m,n-1) and (m,n-2). The first order derivative in the τ - direction incorporates points (m+1,n) and (m-1,n) in place of (m,n) and (m-1,n) and the mixed derivative involves points (m-1,n+1), (m+1,n+1), (m+1,n-1) and (m-1,n-1) in place of points (m,n+1), (m,n-1) (m-1,n-1) and (m-1,n+1). The 11-point molecule would permit larger steps in the τ - direction.

Three different numerical approaches were made for the 11-point molecule computations. The first involved a recurrence relation. The second used the Gauss's Elimination method. The last utilized an iterative finite-difference method. All the three methods failed to give a consistent Δf distribution. A summary of all these methods is included in the Appendices 'A', 'B' and 'D'.

3.2 Solution to the Energy Equation

The energy equation (2.28) is the same as the one used for an accelerated flow problem of Ref. [3]. Consequently, the following solutions, for Pr = 1, may be used.

(1) For the case of no heat transfer at the wall

$$g = 1 + \frac{(\gamma-1)}{2} M_e^2 (1-f'^2) \qquad (3.7)$$

(2) For the case of non-zero wall heat transfer

$$g = 1 + \frac{(\gamma-1)}{2} M_e^2 (f'-f'^2) + (g_w-1)(1-f') \tag{3.8}$$

provided that the wall temperature is kept constant.

3.3 Shearing Stress at the Wall

The shear stress at the wall is given by

$$\tau_w = (\mu \frac{\partial u}{\partial y})_{y=0}$$

$$\tau_w = [\mu \frac{\partial^2 \psi}{\partial \eta^2} (\frac{\partial \eta}{\partial Y})^2 \frac{\partial Y}{\partial y}]_{y=0}$$

Using (2.7), (2.14) and (2.15) one obtains

$$\tau_w = \frac{\mu_w \rho_w}{\rho_\infty} \frac{U_e^{3/2}}{\sqrt{[2\nu_\infty cx]}} f''(0,\tau) \tag{3.9}$$

or

$$\tau_w = \alpha_1 f''(0,\tau) \tag{3.10}$$

where

$$\alpha_1 = \frac{\mu_w \rho_w}{\rho_\infty} \frac{U_e^{3/2}}{\sqrt{[2\nu_\infty cx]}} \tag{3.11}$$

A plot of the shear stress as a function of τ is indicated in Fig. 3.8.

3.4 Heat Transfer at the Wall

The heat transfer at the wall may be obtained from

$$q_w = (-k \frac{\partial T}{\partial y})\Big|_{y=0} \tag{3.12}$$

or

$$q_w = - \frac{k_w h_e}{C_p} g'(0,\tau)(\frac{\partial \eta}{\partial Y} \frac{\partial Y}{\partial y})\Big|_{y=0} \tag{3.13}$$

Differentiating (3.8), one obtains

$$g' = \frac{(\gamma-1)}{2} M_e^2 f''(1-2f') - (g_w-1)f'' \tag{3.14}$$

Using (2.7), (2.14), (2.15) and (3.14) one finds from (3.13)

$$q_w = - \frac{k_w h_e \rho_w}{C_p \rho_\infty} \sqrt{[\frac{U_e}{2\nu_\infty cx}]}\ f''(0,\tau)[\frac{(\gamma-1)}{2} M_e^2 - g_w + 1] \tag{3.15}$$

or

$$q_w = \alpha_2 f''(0,\tau) \tag{3.16}$$

where

$$\alpha_2 = \frac{k_w h_e \rho_w}{C_p \rho_\infty} \sqrt{[\frac{U_e}{2\nu_\infty cx}]}[g_w - 1 - \frac{(\gamma-1)}{2} M_e^2] \tag{3.17}$$

From Fig.3.8 where the shear stress plot as a function of τ is given, the heat transfer at the wall can also be obtained from the relation

$$q_w = \frac{\alpha_2}{\alpha_1}\ \tau_w \tag{3.18}$$

CHAPTER IV

VISCOUS INTERACTIONS

4.1 The Displacement Thickness

Using the relation

$$\nabla\cdot[\rho_e\vec{U}_e\Delta - \int_0^\infty(\rho_e\vec{U}_e - \rho u)dy]$$

$$+ \frac{\partial}{\partial t}[\rho_e\Delta - \int_0^\infty(\rho_e - \rho)dy] = 0 \qquad (4.1)$$

for the unsteady boundary layer as given in reference [19] one may write, for constant ρ_e and constant U_e,

$$\frac{\partial}{\partial t}(\Delta-\delta_\rho) + U_e\frac{\partial}{\partial x}(\Delta-\delta^*) = 0 \qquad (4.2)$$

where

$$\delta^* = \int_0^e(1 - \frac{\rho_u}{\rho_{eU_e}})dy \qquad (4.3)$$

and

$$\delta_\rho = \int_0^e(1 - \frac{\rho}{\rho_e})dy \qquad (4.4)$$

From expression (3.8), one may obtain

$$g-1 = [g_w + \frac{(\gamma-1)}{2} M_e^2 f'](1-f') - (1-f') \tag{4.5a}$$

and

$$g-f' = [g_w + \frac{(\gamma-1)}{2} M_e^2 f'](1-f') \tag{4.5b}$$

Also for the case of no heat transfer $g'(0,\tau) = 0$ and from expression (3.7), one may write

$$g_w = 1 + \frac{(\gamma-1)}{2} M_e^2 \tag{4.6}$$

Using expressions (2.7), (2.14), (4.5a), (4.5b) and (4.6) we may write, following a procedure outlined in Ref. [3], for the case of no heat transfer at the wall

$$\delta^* = \sqrt{[\frac{2\nu_\infty cx}{U_e}]} \int_0^e [1 + \frac{(\gamma-1)}{2} M_e^2 (1+f')](1-f')d\eta \tag{4.7}$$

and

$$\delta_\rho = \sqrt{[\frac{2\nu_\infty cx}{U_e}]} \int_0^e \{[1 + \frac{(\gamma-1)}{2} M_e^2(1+f')](1-f') - (1-f')\}d\eta \tag{4.8}$$

Similarly for the case of non-zero heat transfer at the wall we obtain

$$\delta^* = \sqrt{[\frac{2\nu_\infty cx}{U_e}]} \int_0^e [g_w + \frac{(\gamma-1)}{2} M_e^2 f'](1-f')d\eta \tag{4.9}$$

and

$$\delta_p = \sqrt{\left[\frac{2\nu_\infty\, cx}{U_e}\right]} \int_0^e \{[g_w + \frac{(\gamma-1)}{2} M_e^2 f'](1-f') - (1-f')\}d\eta \qquad (4.10)$$

For the steady state case dependence on time would disappear and as such only the expressions (4.7) and (4.9) would be required with the function f' replaced by its final steady state value f_2' .

4.2 Steady State Boundary Layer Thickness

In order to justify the Prandtl Boundary Layer simplifications, calculations were made for δ/x for the initial and the final steady state.

By definition

$$\rho_e U_e(\delta-\delta^*) = \int_0^e \rho\, u\, dy \qquad (4.11a)$$

or

$$\delta-\delta^* = \int_0^e \frac{\rho u}{\rho_e U_e}\, dy \qquad (4.11b)$$

In terms of the transformed variables

$$\frac{\delta}{x} = \frac{\delta^*}{x} + \frac{1}{x}\sqrt{\left[\frac{2\nu_\infty\, cx}{U_e}\right]} \int_0^e f'd\eta \qquad (4.12)$$

This result may also be expressed in terms of the Hypersonic similarity parameter $\bar{\chi}$ [see equation (4.19)] as:

$$\frac{\delta}{x} = \frac{\delta^*}{x} + \sqrt{2}\,\frac{\bar{\chi}}{M_e^3}\int_0^e f'\,d\eta \tag{4.13}$$

Figure (4.1)* shows the plot of δ/x as a function of $\bar{\chi}$ for the selected cases of zero and non-zero heat transfer at the wall. A plot of $\frac{\delta}{x}/\bar{\chi}$ as a function of M_e ($5 \leq M_e \leq 20$) has also been given in Fig. (4.2) for the case of zero heat transfer at the wall.

4.3 Weak Interaction Induced Pressure

In the acoustic approximation, the pressure rise at the plate surface and the outward velocity of the "displacement plane" may be written [17] as, respectively,

$$\Delta p_v = \rho_e\, a_e v_e \tag{4.14}$$

and

$$v_e = \frac{D\Delta}{Dt} = \frac{\partial \Delta}{\partial t} + U_e\,\frac{\partial \Delta}{\partial x} \tag{4.15}$$

From (4.2), (4.14) and (4.15) we may also write

---

*Curves for CHAPTER IV have been included in Appendix 'F'.

$$\frac{\Delta p_v}{p_e} = \frac{\rho_e a_e}{p_e} \left(\frac{\partial \delta_\rho}{\partial t} + U_e \frac{\partial \delta^*}{\partial x}\right)$$

or

$$\frac{\Delta p_v}{p_e} = \gamma\left(\frac{1}{a_e} \frac{\partial \delta_\rho}{\partial t} + M_e \frac{\partial \delta^*}{\partial x}\right) \tag{4.16}$$

Differentiation of expression (4.9) gives [3]

$$\frac{\partial \delta^*}{\partial x} = \sqrt{\left[\frac{2\nu_\infty C}{U_e}\right]} \left(\frac{I}{2\sqrt{x}} + \sqrt{x} \frac{\partial I}{\partial x}\right) \tag{4.17}$$

where

$$I = \int_0^e [g_w + \frac{(\gamma-1)}{2} M_e^2 f'](1-f')d\eta \tag{4.18}$$

for the case of non-zero wall heat transfer. For the case of no wall heat transfer, expression (4.6) should be used in (4.18)

Using the hypersonic similarity parameter $\bar{\chi}$ [19] defined as

$$\bar{\chi} = M_e^3 \sqrt{\left[\frac{\nu_\infty C}{U_e x}\right]} = M_e^3 \sqrt{\left[\frac{C}{Re_{xe}}\right]} \tag{4.19}$$

and noting that I in expression (4.18) is a function of τ only, we get

$$M_e \frac{\partial \delta^*}{\partial x} = \frac{1}{\sqrt{2}\, M_e^2} \bar{\chi} \left(I - 2\tau \frac{\partial I}{\partial \tau}\right) \tag{4.20}$$

Similarly differentiation of expression (4.10) gives

$$\frac{1}{a_e} \frac{\partial \delta_\rho}{\partial t} = \frac{1}{a_e} \sqrt{\left[\frac{2\nu_\infty Cx}{U_e}\right]} \frac{\partial J}{\partial t} \tag{4.21}$$

where

$$J = \int_0^e \{[g_w + \frac{(\gamma-1)}{2} M_e^2 f'](1-f') - (1-f')\} d\eta \tag{4.22}$$

for the case of non-zero wall heat transfer. For the case of no wall heat transfer one should use expression (4.6) in (4.22).

Noting expression (4.19) and that J is a function of τ only, one may also write

$$\frac{1}{a_e} \frac{\partial \delta_\rho}{\partial t} = \frac{\sqrt{2}}{M_e^2} \bar{\chi} \frac{\partial J}{\partial \tau} \tag{4.23}$$

Substitution of (4.20) and (4.23) in (4.16) yields

$$\frac{\Delta p_v}{p_e} = \frac{\gamma}{M_e^2} \left[\sqrt{2} \frac{\partial J}{\partial \tau} + \frac{1}{\sqrt{2}} \left(I - 2\tau \frac{\partial I}{\partial \tau}\right)\right] \bar{\chi} \tag{4.24}$$

Expression (4.24) has been derived in detail in Ref. [3].

In Ref. [26], parameter λ has been used in place of $\bar{\chi}$, where λ and $\bar{\chi}$ are related by

$$\lambda = a\bar{\chi} \tag{4.25}$$

In the above expression "a" depends primarily on wall temperature for the steady state case.

Our result of expression (4.24) may also be expressed in terms of the parameter λ as:

$$\frac{\Delta p_v}{p_e} = \lambda = a\bar{\chi} \tag{4.26}$$

Here "a" depends on g_w and τ for given γ and M_e.

Expression (4.26) is similar to expression (8) of Ref. [27] where the steady state induced pressure results have been obtained.

For the final steady state we may write, from expression (4.24), as

$$\frac{\Delta p_{v2}}{p_e} = \frac{\gamma I_2}{\sqrt{2}\, M_e^{\,2}}\ \bar{\chi} \tag{4.27}$$

where

$$I_2 = \int_0^e [g_w + \frac{(\gamma-1)}{2} M_e^{\,2} f_2'](1-f_2')d\eta \tag{4.28}$$

for the case of non-zero wall heat transfer. Replacement of g_w in (4.28) by expression (4.6) is essential for the case of no wall heat transfer.

Finally, one obtains the transient contribution to the induced pressure referenced to the final steady state as:

$$\frac{\Delta p}{p_e} = \frac{\Delta p_{v2} - \Delta p_v}{p_e}$$

$$= \frac{\gamma}{M_e^2}\left[\frac{I_2}{\sqrt{2}} - \sqrt{2}\,\frac{\partial J}{\partial \tau} - \frac{1}{\sqrt{2}}\left(I - 2\tau\,\frac{\partial I}{\partial \tau}\right)\right]\bar{\chi} \qquad (4.29)$$

This follows directly from expressions (4.24) and (4.27).

Numerical results for the transient contribution to the pressure distribution have been obtained by programming expression (4.29) on IBM-360/67 Computer. Various results are displayed in Figs. (4.3) through (4.8) in Appendix 'F'.

CHAPTER V

DISCUSSION AND CONCLUSIONS

5.1 Discussion of Results

(1) For zero and non-zero wall heat transfer transient values have been obtained for the shear stress at the wall and the induced pressure distribution in the region downstream of $x = U_e t/1.3$ ($0 \leq \tau \leq 1.3$). The selected results are given in Appendix 'F'.

(2) The stream function increment (Δf) distribution has been given in Figs. 3.3 and 3.4. These distributions have been obtained by taking one percent change in the free stream velocity. The discontinuity in Δf - distribution is noticeable approximately at $\tau = 1.85$ for $\eta = 0.3$, $\tau = 1.65$ for $\eta = 1$, $\tau = 1.4$ for $\eta = 2$, $\tau = 1.3$ for $\eta = 5$.

It should be mentioned that Δf - distribution, for the stepwise-accelerated and decelerated flat plate cases, happens to be identical. Therefore, the results of Ref. [3] may be extended to the range $1 < \tau \leq 1.3$.

(3) The highest order derivative terms (in time and space) of equation (2.31) are

$$(\dot{\Delta f})' = \frac{1}{2(1-\tau f_2')} (\Delta f)''' + \text{---} \qquad (5.1a)$$

or

$$\frac{\partial(\Delta f')}{\partial \tau} = K \frac{\partial^2(\Delta f')}{\partial \eta^2} + \text{---} \qquad (5.1b)$$

Expression (5.1) has the character of the conduction heat equation with the coefficient of conductivity given by

$$K = \frac{1}{2(1-\tau f_2')} \quad . \tag{5.2}$$

In expression (5.2) K would have different signs for $0<\tau<\frac{1}{f_2'}$, and $\frac{1}{f_2'}<\tau<\infty$. At $\tau = \frac{1}{f_2'}$, K would be infinite. It appears that the discontinuity in the Δf - distribution occurs upon approaching the neighbourhood of $\tau = \frac{1}{f_2'}$. A line denoting $\tau = \frac{1}{f_2'}$ is shown in Fig. (3.3).

(4) Some attempts were made (see Appendices 'A', 'B' and 'D') to use the 11-point molecule in place of the 7-point molecule. The 11-point molecule is the result of the commonly used expressions for central derivatives. The results are shown in Fig. A.2 and Fig. B.2. It has been found that the methods incorporating the 11-point molecule are not stable for the equation (2.31) with the associated time and boundary conditions given in section 2.5. The Δf - distribution of Fig. 3.3 and Fig. 3.4 is based on the recurrence relations (3.1), (3.2), and (3.3) incorporating the 7-point molecule. Double precision was used in the computations. Fig. 3.4 shows that Δf is a monotonically increasing function of η for fixed value of τ.

(5) Figures 3.5, 3.6 and 3.7 indicate the satisfaction of the differential equation (2.31) by the stream function increment Δf and its derivatives. The quantity 'd' defined by

$$d = 2(\dot{\Delta f})' + 2\tau[f_2'''(\dot{\Delta f}) - f_2'(\dot{\Delta f})'] - (\Delta f)'''$$

$$- f_2(\Delta f)'' - f_2''(\Delta f) \tag{5.3}$$

has been calculated. The Δf - distribution has been obtained using the 7-point molecule. But in the computation of the quantity 'd', the derivatives based on the 11-point molecule are used. The discrepancies ($d \neq 0$) are the result of this change-over from 7-point molecule to the 11-point molecule. The satisfaction of the differential equation is quite reasonable for large values of η and τ. The discrepancies ($d \neq 0$) are comparable with the highest order derivative $(\Delta f)'''$ for smaller values of η and τ.

As we mentioned previously, the numerical methods incorporating the 11-point molecule have been found unstable for the present problem. It is felt that the results obtained by using the 7-point molecule are quite satisfactory for the estimation of the transient shearing stress and the induced pressures.

(6) In Fig. 3.8 the transient distribution of $\Delta f''(0,\tau)$ is shown. This gives immediately the desired shear stress distribution at the wall. For large values of τ, $\Delta f''(0,\tau)$ appears to approach the final steady state value.

We noted in section 3.4 that the heat transfer at the wall is related to the shear stress at the wall through the Reynolds Analogy:

$$q_w = \frac{\alpha_2}{\alpha_1} \tau_w \qquad (5.4)$$

Therefore, heat transfer at the wall may also be obtained from Fig. 3.8.

(7) The transient contribution to the induced pressure distribution for the case of no heat transfer at the wall is given in Fig. 4.3a. The

transient contribution becomes larger at smaller Mach Numbers and at bigger values of τ . The absolute magnitude of the transient contribution corresponding to $M_e = 5$ is almost equal at $\tau = 1.0$ and larger at $\tau = 0.1$ as compared with the corresponding contribution for the stepwise-accelerated flat plate of Ref. [3]. This may be noticed from the comparison of Figs. 4.3a and 4.3b. Also the contribution is larger at $M_e = 30$ and $\tau = 0.1$ and $\tau = 0.05$ in this case.

In Fig. 4.3c $\frac{\Delta p}{p_e} / \bar{\chi}$ has been plotted as a function of τ. This is a precise form of Fig. 4.3a. One may notice abrupt convexities after $\tau = 1.0$ in this figure. These convexities may indicate that we are soon approaching the vicinity of the "blow-up" region of Δf - distribution.

(8) Figures 4.4a, 4.5a and 4.6a give the transient contribution to the pressure distribution with non-zero heat transfer. In Figures 4.7 and 4.8, some of these results have been further analysed for $\bar{\chi} = 3.5$, $M_e = 10$ and 20 respectively. It is noticed that at a fixed Mach Number and fixed $\bar{\chi}$ the transient contribution is larger for lower values of g_w up to $\tau \simeq 0.18$ whereas the transient contribution is smaller for lower values of g_w in the range $0.18 < \tau < 1.3$. For the case of an adiabatic wall the transient contribution to the pressure distribution is nearly constant as a function of τ up to $\tau = 1$; after $\tau > 1$ the transient contribution increases.

The absolute magnitude of these contributions is found to be larger in the range $0 \leq g_w < 1$ and smaller for $g_w \geq 1$ as compared to the corresponding transient contributions for a stepwise-accelerated flat plate. Figures 4.4b, 4.5b and 4.6b of Ref. [3] have been included for the sake

of comparison.

(9) For a given g_w, given $\bar{\chi}$ and given τ, the transient contribution decreases with the increase in Mach Number. This may be noticed again from Figures 4.4a, 4.5a and 4.6a.

For large Mach Numbers and large values of τ the transient contribution becomes independent of the Mach Number as g_w approaches zero. Figure 4.7 and 4.8 along with Figs. 4.4a, 4.5a and 4.6a may be analysed to indicate this.

Figures 4.4c, 4.5c and 4.6c have been included to reduce the number of curves of the respective Figs. 4.4a, 4.5a and 4.6a.

(10) Now, consider the expression (4.29):

$$\frac{\Delta p}{p_e} = \frac{\gamma}{M_e^2}\left[\frac{1}{\sqrt{2}}(I_2-I) - \sqrt{2}\left(\frac{\partial J}{\partial \tau} - \tau\frac{\partial I}{\partial \tau}\right)\right]\bar{\chi} \qquad (5.5)$$

For the case of no heat transfer at the wall and $0 \leq \tau \leq 1.3$, it has been found that

$$\frac{1}{\sqrt{2}}(I_2-I) >> \sqrt{2}\left(\frac{\partial J}{\partial \tau} - \tau\frac{\partial I}{\partial \tau}\right)$$

and, therefore, one may use the approximate relation

$$\frac{\Delta p}{p_e} = \frac{\gamma}{\sqrt{2}M_e^2}(I_2-I)\,\bar{\chi} \qquad (5.6)$$

which is consistent with the findings of Ref. [3].

For $1 \leq g_w \leq 81$ the contribution of all terms must be considered. However, for $g_w < 1$ and $\tau << 1$, it has been noticed that $\sqrt{2}\,\frac{\partial J}{\partial \tau}$ is the predominant term and for this case we may use the approximate relation

$$\frac{\Delta p}{p_e} = - \frac{\sqrt{2}\,\gamma}{M_e} \frac{\partial J}{\partial \tau}\ \bar{\chi} \tag{5.7}$$

This result is, also, consistent with the corresponding stepwise-accelerated flat plate result of Ref. [3]. The solution in the region $\tau \to 0$, should correspond to that given by Lord Rayleigh [8].

(11) Finally, we justify the use of the Prandtl's Boundary Layer simplifications in the present work. As pointed out by Shen [1], one may use the Prandtl's Boundary Layer equations for the Hypersonic Flows provided $(\frac{\delta}{x})^2 << 1$. Calculations of $\frac{\delta}{x}$ have been made for the initial and the final steady state cases. Some of the limiting results are presented in Figs. 4.1 and 4.2. It has been found that the quantity $(\frac{\delta}{x})^2$ never exceeds 0.3 in the weak interaction rage (i.e. $\bar{\chi} = 0$ to $\bar{\chi} \simeq 3.5$).

5.2 Concluding Remarks

The results, presented in the previous section, have been obtained for the initial zero pressure gradient case and, therefore, are valid for weak interaction induced pressures. The numerical results cover the range $0 \leq \tau \leq 1.3$ and additional attempts should be made to obtain the solution in the region $1 \leq \tau \leq \infty$. It would be convenient to use a parameter α defined by

$$\alpha = \frac{1}{\tau} \tag{5.8}$$

in this range. The solution at $\tau=\alpha=1$ may serve as the additional boundary condition for the region in question.

Once the main aspects of the unsteady flow over a flat plate at zero angle of attack are known for $0 \leq \tau \leq \infty$, it would seem interesting to extend the analysis to include the cases of a wedge, an inclined flat plate, and the circular cone. Further, the problems of strong interaction induced pressure and the oscillating airfoils may be treated.

BIBLIOGRAPHY

1. Shen, S.F., "On the Boundary Layer Equations in Hypersonic Flow", J. Aero. Sci., Vol. 19, July 1952.
2. Lees, L., and Probestein, R.F., "Hypersonic Flows of a Viscous Fluid", United States Air Force Contract No. AF33(038)-250, Project No. 1363, 1953.
3. Rodkiewicz, C.M., "Time Dependent Hypersonic Viscous Interactions", Ph.D. Thesis, Case Institute of Technology, 1967.
4. Bertram, M.H., "Boundary Layer Displacement Effects in Air at Mach Number of 6.8 and 9.6", NACA TN 4133, 1957.
5. Kendall, J.M., Jr., "An Experimental Investigation of Leading Edge Shock-Wave Boundary Layer Interaction at Mach 5.8", J. Aero. Sci., Vol. 24, 1957.
6. Ostrach, S., "Compressible Laminar Boundary Layer and Heat Transfer for Unsteady Motions of a Flat Plate", NACA TN 3569, 1955.
7. Stewartson, K., "On the Impulsive Motion of a Flat Plate in a Viscous Fluid", Quart. Appl. Math. and Mech., 4, 182, 1957.
8. Stewartson, K., "The Theory of Laminar Boundary Layers in Compressible Fluids", Oxford Mathematical Monographs, 1964.
9. Lam, H., and Crocco, L., "Shock Induced Unsteady Laminar Compressible Boundary Layers on a Semi-Infinite Flat Plate", Princeton University Report No. 428, AFOSR TN 58-581, 1958.

10. Mirels, H., "Laminar Boundary Layer Behind Shock Advancing into Stationary Fluid", NACA TN 3401, 1955.

11. Cheng, S.I., "Some Aspects of Unsteady Laminar Boundary Layer Flows", Quart. Appl. Math., Vol. 14, No. 4, January 1957.

12. Kubota, T. and Ko, D.R.S., "A Second Order Weak Interaction Expansion for Moderately Hypersonic Flow Past a Flat Plate", AIAA J. TN, Vol. 5, No. 10, 1967.

13. Cheng, S.I., and Elliot, D., "The Unsteady Laminar Boundary Layer on a Flat Plate", Princeton University Aero. Eng. Report 318, 1955.

14. Lighthill, M.J., "Oscillating Airfoils at High Mach Number", J. Aero. Sci., Vol. 20, June 1953.

15. Landahl, Marten T., "Unsteady Flow Around Thin Wings at High Mach Numbers", J. Aero. Sci., Vol. 24, January 1957.

16. Miles, J.W., "Unsteady Flow at Hypersonic Speeds in Collar A.R. and Tinkler, J. eds., Hypersonic Flow", Academic Press, pp. 185-197, 1960.

17. Moore, F.K., "Hypersonic Boundary Layer Theory", in F.K. Moore, ed. "Theory of Laminar Flows, High Speed Aerodynamics and Jet Propulsion", Vol. IV, Princeton University Press, 1964.

18. Sears, "Theory of Time-Dependent Laminar Flows", in F.K. Moore, ed. "Theory of Laminar Flows, High Speed Aerodynamics and Jet Propulsion", Vol. IV, Princeton University Press, 1964.

19. Moore, F.K., and Ostrach, S., "Displacement Thickness of the Unsteady Boundary Layer", J. Aero. Sci., January 1957.

20. Hays, W.D., and Probestein, R.F., "Hypersonic Flow Theory", Academic Press, 1959.

21. Goldstein, Sydney, "Modern Developments in Fluid Dynamics", Vol. 1, Clarenden Press (Oxford), 1938.

22. Moore, F.K., "Unsteady Laminar Boundary Layer Flow", NACA TN 2471, 1951.

23. Schuh, H., "Calculation of Unsteady Boundary Layers in Two Dimensional Flow", Zeitschr Flugw. Vol. 1, pp. 122-131, 1953.

24. Bruce, G., Peaceman, D., Rachford, H., and Rice, J., "Calculation of Unsteady State Gas Flow Through Porous Media", Petroleum Trans., A.I.M.E., 198,79, 1953.

25. Garabedian, P.R., "Partial Differential Equations", John Wiley, New York, 1964.

26. White Jr., F.M., "Hypersonic Laminar Viscous Interactions on Inclined Flat Plates", ARS Journal, pp. 780-781, May 1962.

27. Bertram, M.H. and Blackstock, T.A., "Some Solutions to the Problem of Predicting Boundary-Layer Self-Induced Pressures". NASA TN D-798, April 1961.

28. Stanton, R.G., "Numerical Methods for Science and Engineering", Prentice-Hall, 1962.

29. Lapidus, L., "Digital Computation for Chemical Engineers", McGraw-Hill, 1962.

APPENDIX 'A'

RECURRENCE RELATIONS INVOLVING THE 11-POINT MOLECULE

A.1 Formation of the Difference Equation

For zero pressure gradient we have from equation (2.31):

$$2(\dot{\Delta f})' + 2\tau[f_2''(\dot{\Delta f}) - f_2'(\dot{\Delta f})'] - \Delta f''' - f_2(\Delta f)'' - f_2''(\Delta f) = 0 \qquad (A.1)$$

or

$$2\dot{S}'+2\tau(f_2''\dot{S}-f_2'\dot{S}')-S'''-f_2S''-f_2''S = 0 \qquad (A.2)$$

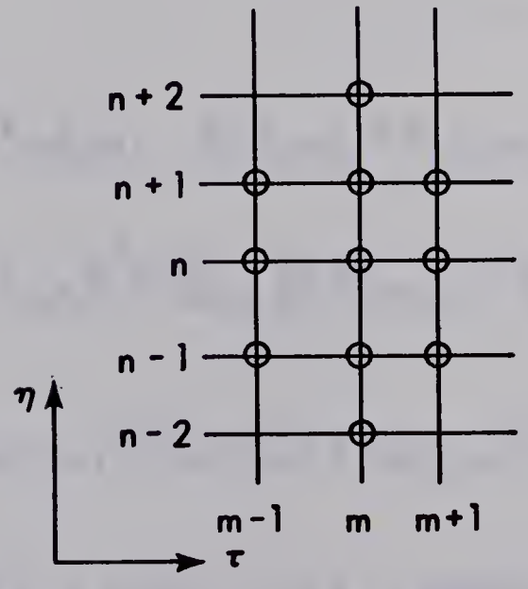

Fig. A.1

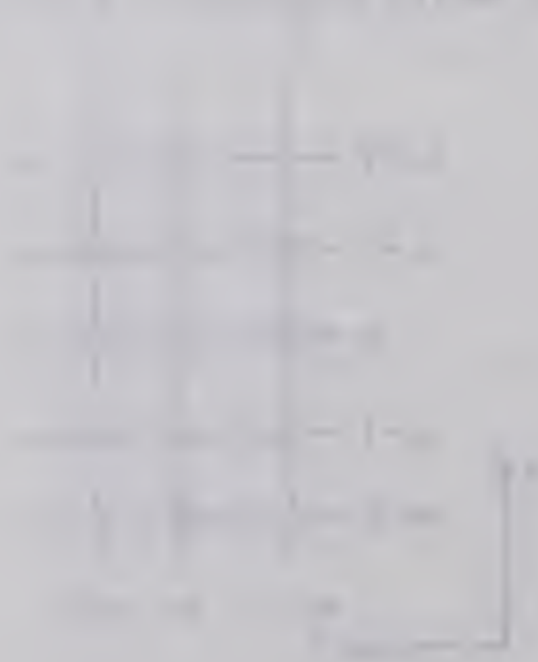

Let H and T be the elementary step magnitudes in η and τ directions respectively. Then [28] we may write

$$\dot{S} = \frac{1}{2T} (S_{m+1,n} - S_{m-1,n}) \tag{A.3}$$

$$S' = \frac{1}{2H} (S_{m,n+1} - S_{m,n-1}) \tag{A.4}$$

$$S'' = \frac{1}{H^2} (S_{m,n+1} - 2S_{m,n} + S_{m,n-1}) \tag{A.5}$$

$$S''' = \frac{1}{2H^3} (S_{m,n+2} - 2S_{m,n+1} + 2S_{m,n-1} - S_{m,n-2}) \tag{A.6}$$

$$\dot{S}' = \frac{1}{4HT} (S_{m+1,n+1} - S_{m-1,n+1} + S_{m-1,n-1} - S_{m+1,n-1}) \tag{A.7}$$

Substituting (A.3) through (A.7) into expression (A.2), we obtain

$$H^2 (S_{m+1,n+1} - S_{m-1,n+1} + S_{m-1,n-1} - S_{m+1,n-1})$$

$$+ 4 \tau_{m,n} H^3 T[f''_{2m,n} \frac{1}{2T} (S_{m+1,n} - S_{m-1,n}) - f'_{2m,n} \frac{1}{4HT} (S_{m+1,n+1}$$

$$- S_{m-1,n+1} + S_{m-1,n-1} - S_{m+1,n-1})] - T(S_{m,n+2} - 2S_{m,n+1}$$

$$+ 2S_{m,n-1} - S_{m,n-2}) - f_{2m,n} 2HT(S_{m,n+1} - 2S_{m,n} + S_{m,n-1})$$

$$- f''_{2m,n} 2H^3 T S_{m,n} = 0 \tag{A.8}$$

A.2 Derivation of the Recurrence Relations

Expression (A.8) can also be written in the following general form

$$a_{m,n}\, S_{m+1,n+1} + b_{m,n}\, S_{m+1,n} + c_{m,n}\, S_{m+1,n-1} = d_{m,n} \qquad (A.9)$$

where

$$a_{m,n} = (1-\tau_{m,n} f'_{2m,n})\, H^2 \qquad (A.10)$$

$$b_{m,n} = 2f'''_{2m,n}\, \tau_{m,n}\, H^3 \qquad (A.11)$$

$$c_{m,n} = -\,(1-\tau_{m,n} f'_{2m,n})\, H^2 \qquad (A.12)$$

$$\begin{aligned} d_{m,n} = {} & T(S_{m,n+2} - 2S_{m,n+1} + 2S_{m,n-1} - S_{m,n-2}) \\ & + 2HTf_{2m,n}\,(S_{m,n+1} - 2S_{m,n} + S_{m,n-1}) \\ & + 2H^3 T f'''_{2m,n}\, S_{m,n} + (1-\tau_{m,n} f'_{2m,n})\, H^2\,(S_{m-1,n+1} - S_{m-1,n-1}) \\ & + 2H^3 \tau_{m,n} f'''_{2m,n}\, S_{m-1,n} \end{aligned} \qquad (A.13)$$

Considering the boundary conditions in conjunction with (A.9) a recurrence formula can be obtained, namely,

$$a_{m,n}\, S_{m+1,n+1} + b'_{m,n}\, S_{m+1,n} = d'_{m,n} \qquad (A.14)$$

where

$$b'_{m,n} = b_{m,n} - c_{m,n}\, \frac{a_{m,n-1}}{b'_{m,n-1}} \quad ; \quad n>3 \qquad (A.15)$$

and

$$d'_{m,n} = d_{m,n} - c_{m,n}\, \frac{d'_{m,n-1}}{b'_{m,n-1}} \quad ; \quad n>3 \qquad (A.16)$$

and where for n = 3 we have from the boundary conditions

$$b'_{m,3} = b_{m,3} + \frac{1}{4}\, c_{m,3} \qquad (A.17)$$

$$d'_{m,3} = d_{m,3} \qquad (A.18)$$

Having initial $b'_{m,n-1}$ and $d'_{m,n-1}$ we can find from (A.15) and (A.16) all $b'_{m,n}$ and $d'_{m,n}$ respectively. With these values we can obtain from (A.14) variable $S_{m+1,n}$ provided that we have $S_{m+1,n+1}$.

Let n = N represent the location for which "e" condition prevails. We know at this location from the north boundary condition that

$$\frac{\partial S}{\partial \eta} = \frac{1}{2\Delta\eta}\,(-3S_1 + 4S_2 - S_3) = 0 \qquad (A.19)$$

Therefore,

$$- 3S_{m+1,N} + 4S_{m+1,N-1} - S_{m+1,N-2} = 0 \qquad (A.20)$$

Also from (A.14) one may write

$$a_{m,N-1}\, S_{m+1,N} + b'_{m,N-1}\, S_{m+1,N-1} = d'_{m,N-1} \qquad (A.21a)$$

and

$$a_{m,N-2}\, S_{m+1,N-1} + b'_{m,N-2}\, S_{m+1,N-2} = d'_{m,N-2} \qquad (A.22a)$$

From (A.22a) one obtains

$$S_{m+1,N-2} = \frac{d'_{m,N-2}}{b'_{m,N-2}} - \frac{a_{m,N-2}}{b'_{m,N-2}}\, S_{m+1,N-1} \qquad (A.22b)$$

Substituting (A.22b) into (A.20) we have

$$3S_{m+1,N} - 4S_{m+1,N-1} + \frac{d'_{m,N-2}}{b'_{m,N-2}} - \frac{a_{m,N-2}}{b'_{m,N-2}}\, S_{m+1,N-1} = 0 \qquad (A.23)$$

From (A.21a) we have

$$S_{m+1,N-1} = \frac{d'_{m,N-1}}{b'_{m,N-1}} - \frac{a_{m,N-1}}{b'_{m,n-1}}\, S_{m+1,N} \qquad (A.21b)$$

Substituting (A.21b) into (A.23) one finally obtains

$$3S_{m+1,N} - 4\frac{d'_{m,N-1}}{b'_{m,N-1}} + 4\frac{a_{m,N-1}}{b'_{m,N-1}}S_{m+1,N}$$

$$+\frac{d'_{m,N-2}}{b'_{m,N-2}} - \frac{a_{m,N-2}}{b'_{m,N-2}}\left(\frac{d'_{m,N-1}}{b'_{m,N-1}} - \frac{a_{m,N-1}}{b'_{m,N-1}}S_{m+1,N}\right) = 0 \qquad \text{(A.24a)}$$

or

$$S_{m+1,N} = \frac{4\frac{d'_{m,N-1}}{b'_{m,N-1}} - \frac{d'_{m,N-2}}{b'_{m,N-2}} + \frac{a_{m,N-2}}{b'_{m,N-2}}\frac{d'_{m,N-1}}{b'_{m,N-1}}}{3 + 4\frac{a_{m,N-1}}{b'_{m,N-1}} + \frac{a_{m,N-2}}{b'_{m,N-2}}\frac{a_{m,N-1}}{b'_{m,N-1}}} \qquad \text{(A.24b)}$$

The above expression constitutes the starting point in the use of expression (A.14).

Expressions (A.14) through (A.18) and (A.24) were programmed on IBM-360/67 computer. Results are shown in Fig. A.2. Values of Δf for $\tau = 0$ have been calculated from the initial condition (2.37) prescribed for the problem. Recurrence relations (3.1), (3.2), and (3.3) have been used to calculate Δf for $\tau = 0.05$ (or m=2). For $\tau = 0.1$ (or m=3) Δf has been calculated using the recurrence relations (A.14) through (A.18) and (A.24). After $\tau = 0.1$, the method described in this appendix becomes unstable. The values of Δf, obtained for $\tau = 0.1$, are about 0.15% higher (for $\eta = 1.0$ and $\eta = 5.0$) than the corresponding values obtained by using the recurrence relations (3.1), (3.2), and (3.3).

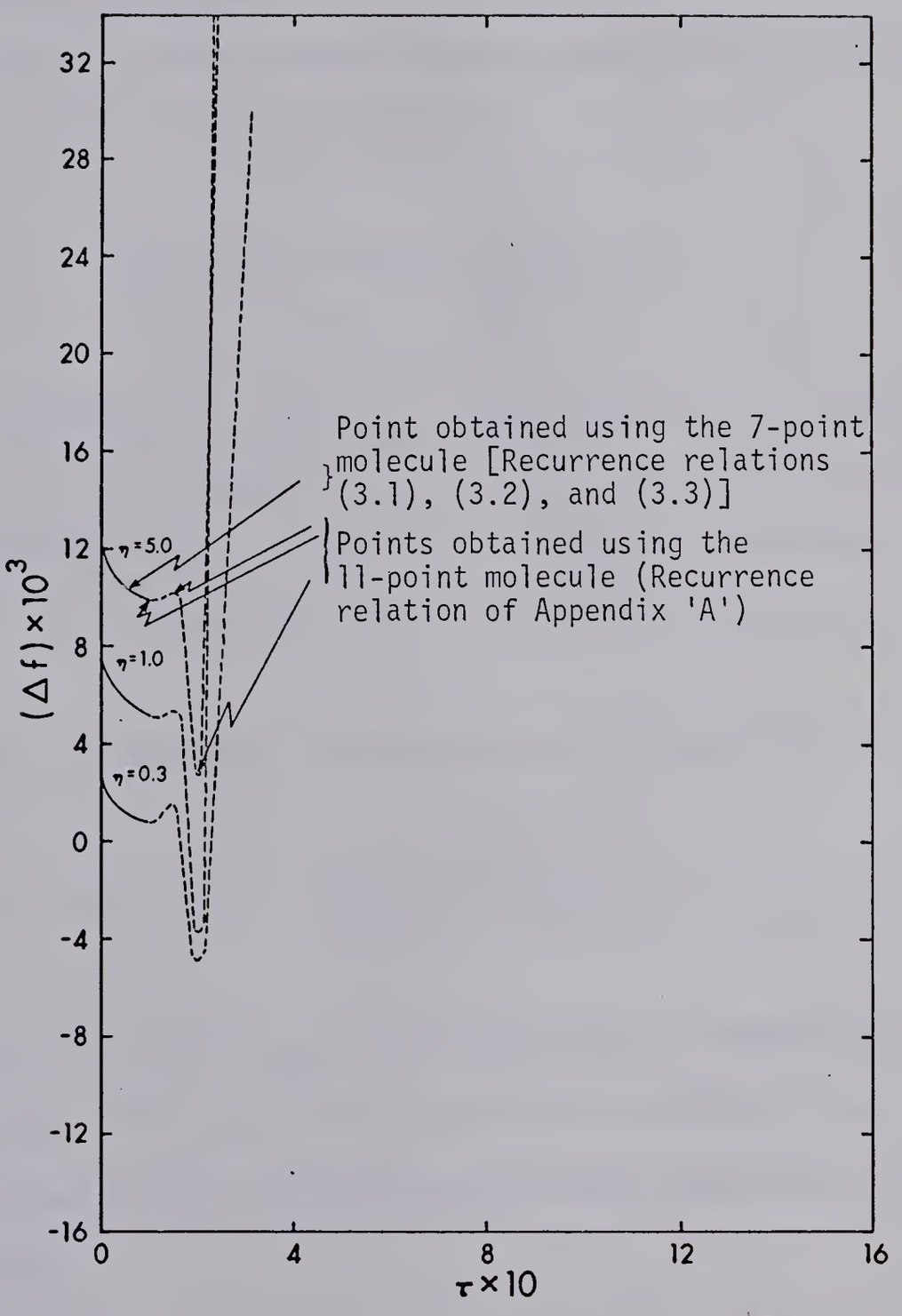

Fig. A.2 Stream Function Increment (Δf) Distribution Curve

A.3 Reasons for the Unstability

When a search was made to find out the causes for the unstability, it was noticed to be associated with the expressions (A.15) through (A.18). From expression (A.17) it may be noted that the coefficient of $c_{m,3}$ is 1/4. Also one may write from (A.15) and (A.17) as:

$$b'_{m,4} = b_{m,4} + c_{m,4} \left(- \frac{a_{m,3}}{b_{m,3} + \frac{1}{4} c_{m,3}}\right) \qquad (A.25)$$

In the above expression $b_{m,3}$ and $b_{m,4}$ are of the order of 0.000095 or smaller for $\tau = 0.10$ whereas $a_{m,3}$ and $c_{m,3}$ are of the order of 0.00995 or smaller and $c_{m,3} = - a_{m,3}$. For a rough estimate of the coefficient of $c_{m,4}$, we may drop $b_{m,3}$ and we find the coefficient to be 4.

Again, one may obtain from expressions (A.15) and (A.25)

$$b'_{m,5} = b_{m,5} + c_{m,5} \left(- \frac{a_{m,4} b_{m,3} + \frac{1}{4} a_{m,4} c_{m,3}}{b_{m,3} b_{m,4} + \frac{1}{4} b_{m,4} c_{m,3} - a_{m,3} c_{m,4}}\right) \qquad (A.26)$$

Here also $b_{m,3}$, $b_{m,4}$ and $b_{m,5}$ are of the order of 0.000095 whereas $c_{m,3}$, $c_{m,4}$, $a_{m,3}$ and $a_{m,4}$ are of the order of 0.00995 with $c_{m,n} = -a_{m,n}$. Neglecting the smaller order terms we may obtain the coefficient of $c_{m,5}$, approximately, as

$$\frac{1}{4} \frac{a_{m,4}\ c_{m,3}}{a_{m,3}\ c_{m,4}}$$

which gives 1/4.

Thus, we find that the coefficient of $c_{m,n}$ in the recurrence relation (A.15) fluctuates between 1/4 and 4. This causes fluctuations in the value of $b'_{m,n}$ and $d'_{m,n}$ and consequently the $S_{m,n}$ values obtained from (A.14) fluctuate. There are no fluctuations in the values of $a_{m,n}$.

It was felt that the unstability in using the full molecule may be associated with the recurrence relations used and, therefore, the Gauss's Elimination method was tried. This has been described in Appendix 'B'. However, the unstability was noticed with the Gauss's Elimination method also. A third method described in Appendix 'D' did not give any satisfactory results either. It is thought that the 11-point molecule is not suitable for the computations of $S_{m,n}$ of equation (A.9).

APPENDIX 'B'

GAUSS'S ELIMINATION METHOD

B.1 Formation of the Problem in a Tridiagonal System

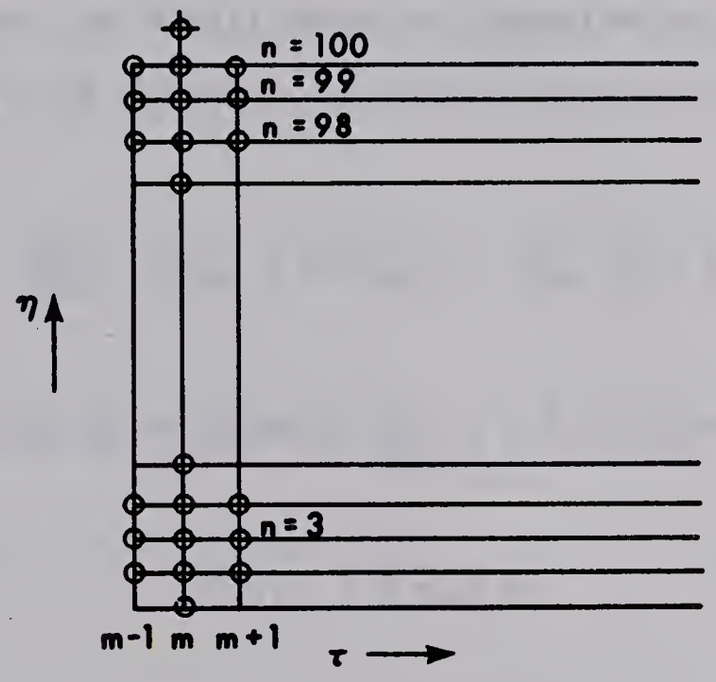

Fig. B.1

The Gauss's Elimination Method has been used to solve the equation

$$a_{m,n}\, S_{m+1,n+1} + b_{m,n}\, S_{m+1,n} + c_{m,n}\, S_{m+1,n-1} = d_{m,n} \qquad (B.1)$$

derived in Appendix 'A' [see equation (A.9)].

The associated boundary conditions are (see section 2.5):

$$\frac{\partial S_{m+1,1}}{\partial \eta} = 0 = S_{m+1,1}$$

(B.2)

and

$$\frac{\partial S_{m+1,100}}{\partial \eta} = 0$$

In addition we have the initial condition prescribed by (2.37).

The first of the two south boundary conditions implies

$$\frac{1}{2\Delta\eta} (-3S_{m+1,1} + 4S_{m+1,2} - S_{m+1,3}) = 0$$

and using the second south boundary, $S_{m+1,1} = 0$, we have

$$S_{m+1,2} = \frac{1}{4} S_{m+1,3} \tag{B.3}$$

With $n = 3$, we obtain from equation (B.1)

$$a_{m,3} S_{m+1,4} + b_{m,3} S_{m+1,3} + c_{m,3} S_{m+1,2} = d_{m,3}$$

In view of relation (B.3), it becomes

$$a_{m,3} S_{m+1,4} + (b_{m,3} + \frac{1}{4} c_{m,3}) S_{m+1,3} = d_{m,3} \tag{B.4}$$

With $n = 4,5,\ldots, 97, 98$, one obtains from (B.1)

$$\left.\begin{aligned} a_{m,4}\, S_{m+1,5} + b_{m,4}\, S_{m+1,4} + c_{m,4}\, S_{m+1,3} &= d_{m,4} \\ a_{m,5}\, S_{m+1,6} + b_{m,5}\, S_{m+1,5} + c_{m,5}\, S_{m+1,4} &= d_{m,5} \\ \vdots \\ a_{m,97}\, S_{m+1,98} + b_{m,97}\, S_{m+1,97} + c_{m,97}\, S_{m+1,96} &= d_{m,97} \\ a_{m,98}\, S_{m+1,99} + b_{m,98}\, S_{m+1,98} + c_{m,98}\, S_{m+1,97} &= d_{m,98} \end{aligned}\right\} \quad (B.5)$$

The north boundary condition gives

$$S_{m+1,100} = \frac{1}{3}\,(4S_{m+1,99} - S_{m+1,98}) \qquad (B.6)$$

and expression (B.1) with $n = 99$ gives

$$a_{m,99}\, S_{m+1,100} + b_{m,99}\, S_{m+1,99} + c_{m,99}\, S_{m+1,98} = d_{m,99}$$

Using (B.6), we obtain

$$\left(\frac{4}{3}\, a_{m,99} + b_{m,99}\right) S_{m+1,99} + \left(c_{m,99} - \frac{1}{3}\, a_{m,99}\right) S_{m+1,98} = d_{m,99} \qquad (B.7)$$

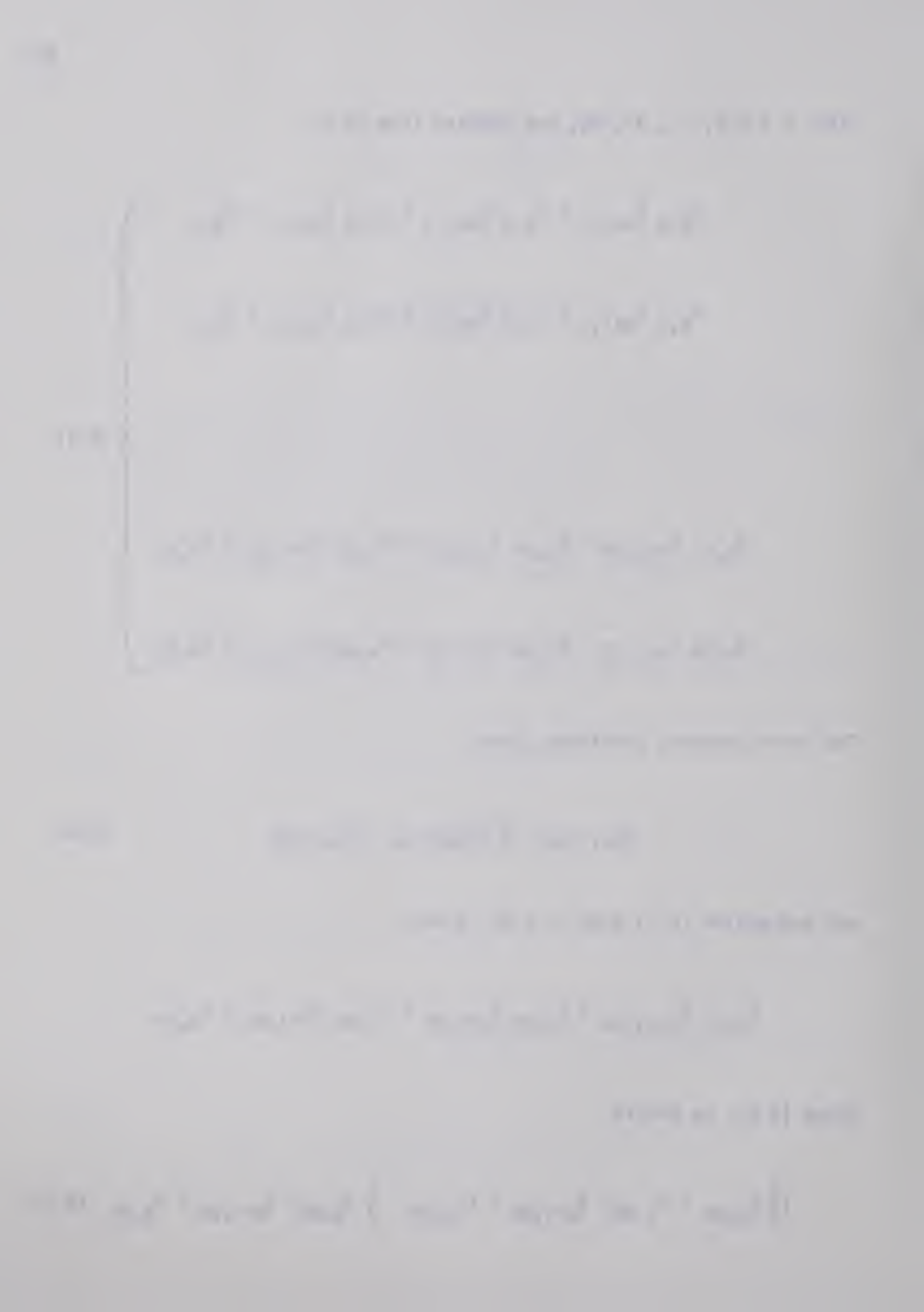

In this manner we obtain 97 equations and 97 unknowns, namely, $S_{m+1,3}, \ldots, S_{m+1,99}$. Putting the equations (B.4), (B.5) and (B.7) in the matrix form, we find

$$\begin{bmatrix} b_{m,3} + \frac{1}{4} c_{m,3} & a_{m,3} & & & & & \\ c_{m,4} & b_{m,4} & a_{m,4} & & & & \\ & \ddots & \ddots & \ddots & & & \\ & & & & & & \\ & & & c_{m,98} & b_{m,98} & a_{m,98} & \\ & & & & c_{m,99} - \frac{1}{3} a_{m,99} & \frac{4}{3} a_{m,99} + b_{m,99} & \end{bmatrix} \begin{bmatrix} S_{m+1,3} \\ S_{m+1,4} \\ S_{m+1,5} \\ \vdots \\ S_{m+1,97} \\ S_{m+1,98} \\ S_{m+1,99} \end{bmatrix} = \begin{bmatrix} d_{m,3} \\ d_{m,4} \\ \\ \vdots \\ d_{m,97} \\ d_{m,98} \\ d_{m,99} \end{bmatrix} \tag{B.8}$$

B.2 Gauss Elimination for a Tridiagonal System

In the previous section we obtained a system of 97 linear algebraic equations of the form

$$B_3 S_3 + C_3 S_4 = D_3$$

$$A_i S_{i-1} + B_i S_i + C_i S_{i+1} = D_i; \; i=4,\ldots,N-1 \tag{B.9}$$

$$A_N S_{N-1} + B_N S_N = D_N; \; N = 99$$

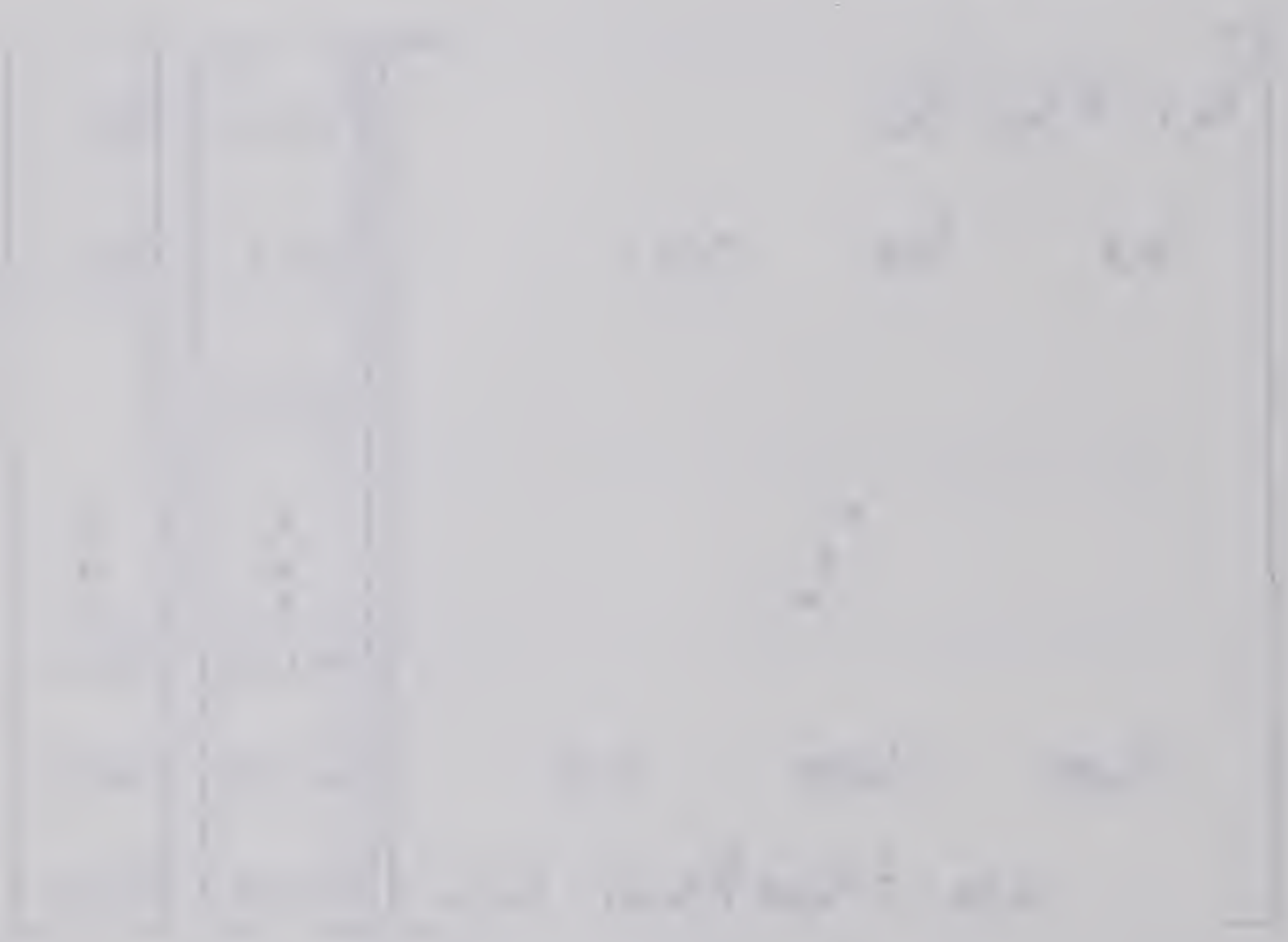

where the S_i are unknown and where the A_i, B_i, C_i and D_i are given coefficients. Since the coefficient matrix of the system is tridiagonal, i.e. has no non-zero elements except on the main diagonal and on the diagonals adjacent to the main diagonal, there is a very simple algorithm for solving the equations. It was first used in connection with parabolic partial differential equations by Bruce, Peaceman, Rachford and Rice [24]. In this algorithm, which is actually just the Gauss's Elimination method, the number of arithmatic operations is proportional to N as compared to $\frac{1}{3}N^3$ for the general matrix.

The S_i as defined by expression (B.9) can be written out explicitly through use of the following formulas:

$$b_3^* = \frac{C_3}{B_3}\ ,\ b_i^* = \frac{C_i}{B_i - A_i\ b_{i-1}^*}\ ,\ i=4,5,\ldots,N-1$$

$$q_3^* = \frac{D_3}{B_3}\ ,\ q_i^* = \frac{D_i - A_i\ q_{i-1}^*}{B_i - A_i\ b_{i-1}^*}\ ,\ i=4,5,\ldots,N-1 \qquad \text{(B.10)}$$

With these coefficients the unknown S_i are given by

$$S_N = q_N^*$$

$$S_i = q_i^* - b_i^*\ S_{i+1}\ ,\ i=N-1,N-2,\ldots,3. \qquad \text{(B.11)}$$

The values of S_i obtained by using this particular method are shown in Fig. B.2. Initial condition (2.37) prescribes the value of S_i(or Δf) for $\tau=0$. For $\tau=0.05$ and $\tau=0.1$, the value of S_i have been

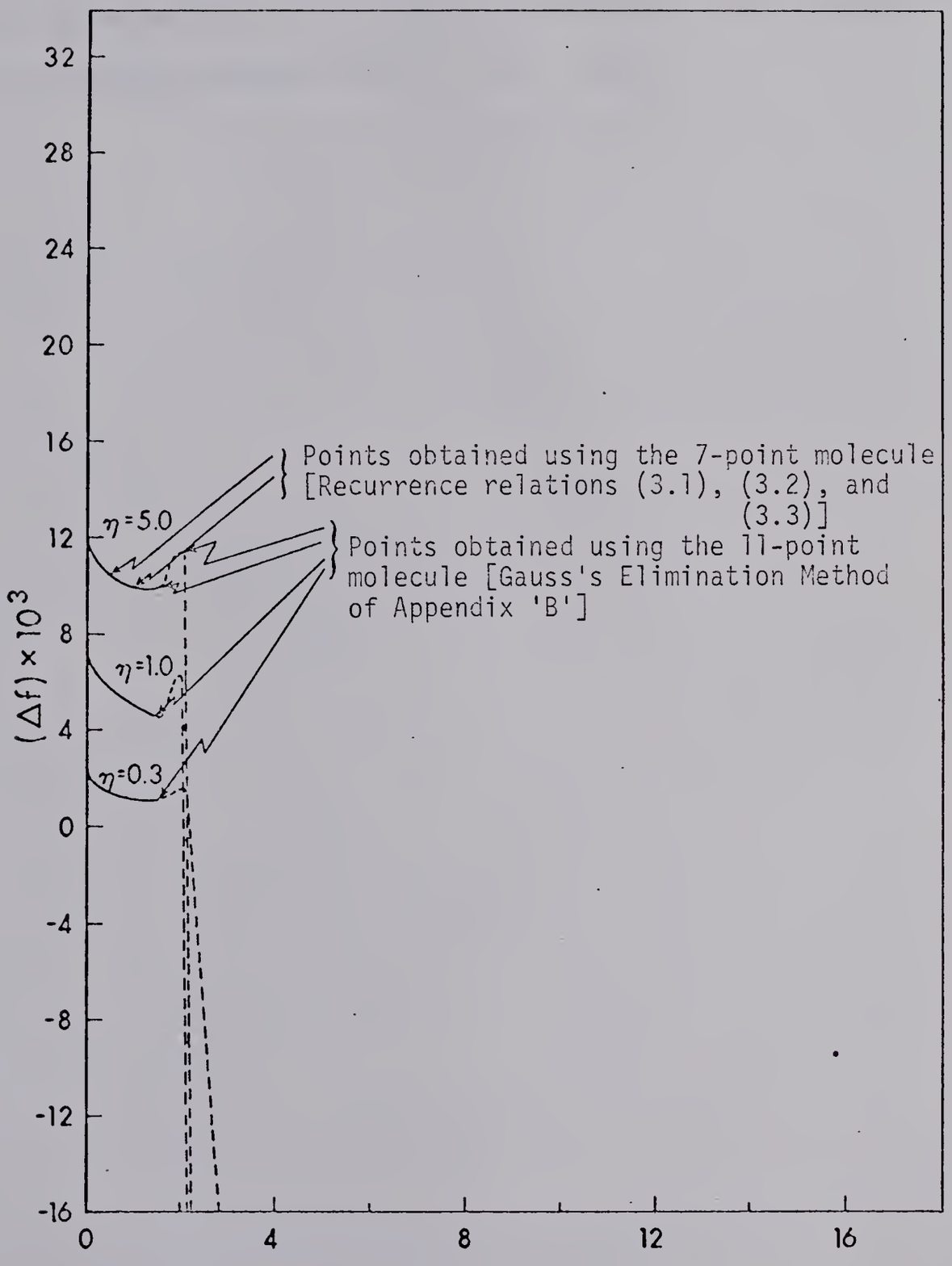

Fig. B.2 Stream Function Increment (Δf) Distribution Curve

obtained from the recurrence relations (3.1), (3.2), and (3.3). Gauss's method gives the value for $\tau \geq 0.15$. We notice from the figure that the method of this appendix becomes unstable after $\tau = 0.15$.

APPENDIX 'C'

ITERATIVE FINITE DIFFERENCE METHOD INVOLVING THE 7-POINT MOLECULE

C.1 Formation of the Difference Equation

The iterative finite difference method has been developed to solve equation (2.31). The finite difference approximations involve the 7-point molecule.

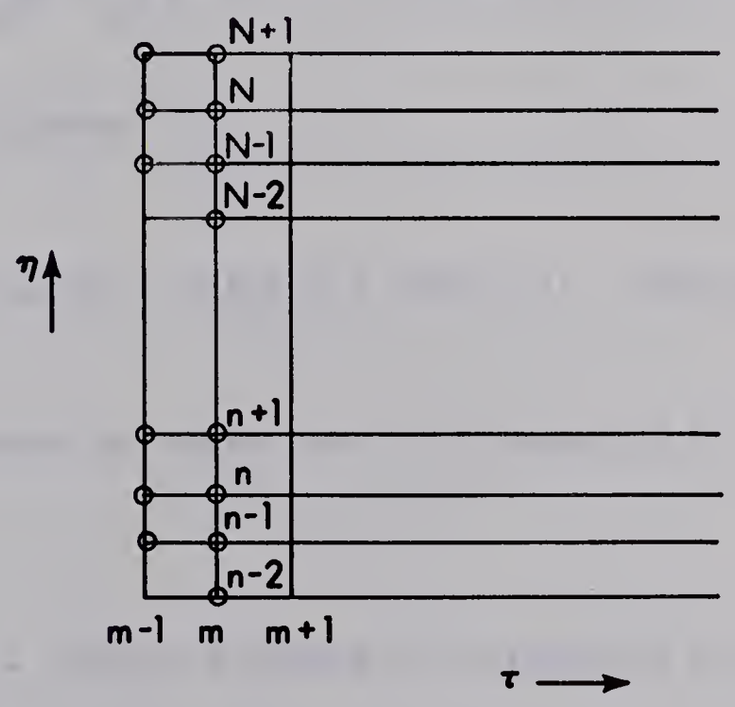

Fig. C.1

If H and T denote elementary step magnitudes in η and τ direction, then one may write [29]

$$\frac{\partial \Delta f}{\partial \tau} = \frac{1}{T} [\Delta f(m,n) - \Delta f(m-1,n)] \qquad (C.1)$$

$$\frac{\partial \Delta f}{\partial \eta} = \frac{1}{2H} [\Delta f(m,n+1) - \Delta f(m,n-1)] \qquad (C.2)$$

$$\frac{\partial^2 \Delta f}{\partial \eta \partial \tau} = \frac{1}{2HT} [\Delta f(m,n+1) - \Delta f(m,n-1) - \Delta f(m-1,n+1) + \Delta f(m-1,n-1)] \qquad (C.3)$$

$$\frac{\partial^2 \Delta f}{\partial \eta^2} = \frac{1}{H^2} [\Delta f(m,n+1) - 2\Delta f(m,n) + \Delta f(m,n-1)] \qquad (C.4)$$

and using Taylor's Series

$$\frac{\partial^3 \Delta f}{\partial \eta^3} = \frac{1}{H^3} [\Delta f(m,n+1) - 3\Delta f(m,n) + 3\Delta f(m,n-1) - \Delta f(m,n-2)] \qquad (C.5)$$

Substitution of expressions (C.1) through (C.5) into (2.31) yields:

$$T(\Delta f(m,n+1) - 3\Delta f(m,n) + 3\Delta f(m,n-1) - \Delta f(m,n-2)] + HTf_2(m,n) \times [\Delta f(m,n+1) - 2\Delta f(m,n) + \Delta f(m,n-1)] + H^3 T f_2'(m,n)\Delta f(m,n)$$

$$= H^2[1-\tau_m f_2'(m,n)] \times [\Delta f(m,n+1) - \Delta f(m,n-1) - \Delta f(m-1,n+1) + \Delta f(m-1,n-1)] + 2H^3 \tau_m f_2'(m,n)[\Delta f(m,n) - \Delta f(m-1,n)] \qquad (C.6)$$

Writing (C.6) in the general form, one obtains

$$a_{m,n}S_{m,n+1} + b_{m,n}S_{m,n} + c_{m,n}S_{m,n-1} + d_{m,n}S_{m,n-2} = e_{m,n} \qquad (C.7a)$$

or

$$S_{m,n} = \frac{e_{m,n} - (a_{m,n}S_{m,n+1} + c_{m,n}S_{m,n-1} + d_{m,n}S_{m,n-2})}{b_{m,n}} \qquad (C.7b)$$

where

$$a_{m,n} = T + HTf_2(m,n) - H^2[1-\tau_m f_2'(m,n)] \qquad (C.8)$$

$$b_{m,n} = -3T - 2HTf_2(m,n) + H^3Tf_2''(m,n)$$

$$- 2H^3\tau_m f_2''(m,n) \qquad (C.9)$$

$$c_{m,n} = 3T + HTf_2(m,n) + H^2[1-\tau_m f_2'(m,n)] \qquad (C.10)$$

$$d_{m,n} = -T$$

$$e_{m,n} = H^2[1-\tau_m f_2'(m,n)][S_{m-1,n-1} - S_{m-1,n+1}]$$

$$= 2H^3\tau_m f_2''(m,n)\, S_{m-1,n} \qquad (C.11)$$

The associated boundary conditions with the equation (2.31) are:

$$\frac{\partial S_{m,100}}{\partial \eta} = 0 = \frac{1}{2\Delta\eta}\left(-3S_{m,100} + 4S_{m,99} - S_{m,98}\right) \qquad (C.12)$$

$$\frac{\partial S_{m,1}}{\partial \eta} = 0 = \frac{1}{2\Delta\eta}\left(-3S_{m,1} + 4S_{m,2} - S_{m,3}\right) \qquad (C.13)$$

$$S_{m,1} = 0 \qquad (C.14)$$

The initial values of $S_{m,n}$ may be obtained from (2.37).

In the above expressions, n = 100 represents the location for which "e" condition prevails.

C.2 Iterative Finite Difference Method

In this method, one assumes the values of the function and then corrects those values with the help of the differential equation in the finite difference form and the associated boundary conditions.

To start with, one may assume the same values of $S_{m,n}$ in the second column of Fig. C.1 as those in the previous column [The values of $S_{m,n}$ in the first column will be given by the initial condition (2.37)]. Using (C.7b), (C.12), (C.13) and (C.14) the values of $S_{m,n}$ so assumed can be suitably iterated to obtain the "exact" values of the function $S_{m,n}$ in the second column correct to the desired degree of accuracy. In obtaining the values of Fig. C.2, error was driven out of the sixth place after the decimal point in the value of $S_{m,n}$. The computation time increases rapidly

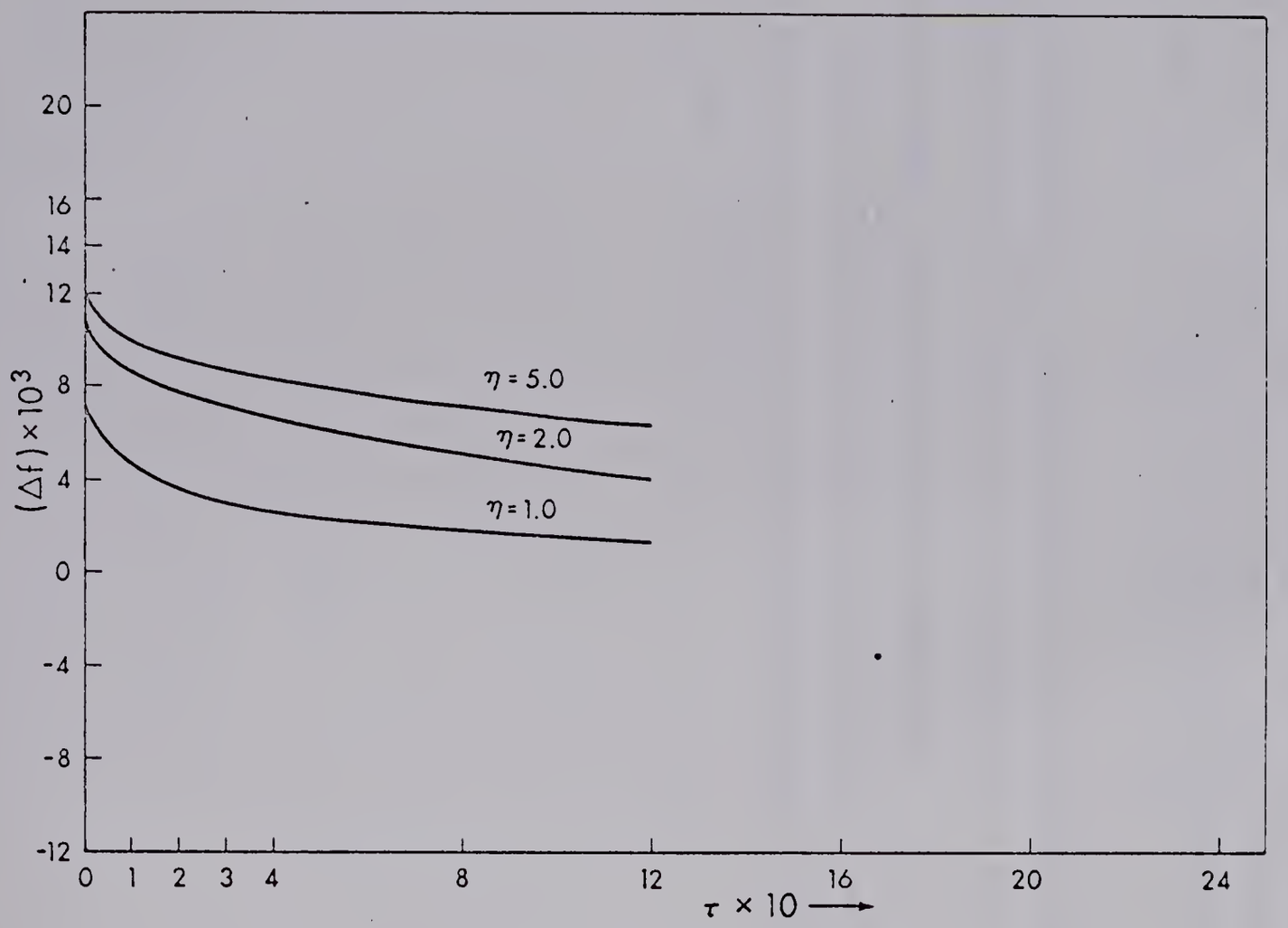

Fig. C.2 Stream Function Increment (Δf) Distribution Curve
(Iterative Finite-Difference Method of Appendix 'C')

as we want to drive the error out of the seventh place after the decimal point.

Having obtained the values in the second column, one may proceed to obtain the values of $S_{m,n}$ in the third column. This marching forward procedure in association with the iterative technique may be used for the successive columns and the error may be driven out of all the 8-places after the decimal point (in single precision) depending upon the accuracy desired.

The values of $S_{m,n}$ obtained (see Fig. C.2) using this method are about 4% higher (at τ=1) as compared with the values of Fig. 3.3*. The present method happens to be costly computer time-wise.

Finally, it should be mentioned that this numerical method would prove most effective for functions which decay more rapidly with time than the function under consideration.

*See Appendix 'F'

APPENDIX 'D'

ITERATIVE FINITE DIFFERENCE METHOD INVOLVING THE 11-POINT MOLECULE

An iterative finite difference method similar to Appendix 'C' was also tried for the full molecule consisting of 11-points.

Rewriting equation (A.8) of Appendix 'A' in the general form as shown below, one finds

$$A_{m,n}S_{m,n+2} + B_{m,n}S_{m,n+1} + C_{m,n}S_{m,n} + D_{m,n}S_{m,n-1}$$

$$+ E_{m,n}S_{m,n-2} = F_{m,n} \qquad (D.1)$$

where

$$A_{m,n} = T \qquad (D.2)$$

$$B_{m,n} = -2T + 2HT\, f_{2m,n} \qquad (D.3)$$

$$C_{m,n} = -4HT\, f_{2m,n} + 2H^3T\, f''_{2m,n} \qquad (D.4)$$

$$D_{m,n} = 2T + 2HT\, f_{2m,n} \qquad (D.5)$$

$$E_{m,n} = -T \tag{D.6}$$

$$F_{m,n} = (1-\tau_{m,n}f'_{2m,n})H^2(S_{m+1,n+1}-S_{m+1,n-1})$$

$$+ 2H^3\tau_{m,n}f''_2S_{m+1,n} - (1-\tau_{m,n}f'_{2m,n})\,H^2$$

$$x\,(S_{m-1,n+1} - S_{m-1,n-1}) - 2H^3\tau_{m,n}f'''_{2m,n}S_{m-1,n} \tag{D.7}$$

Equation (D.1) may also be written as

$$S_{m,n} = \frac{F_{m,n}-(D_{m,n}S_{m,n-1}-E_{m,n}S_{m,n-2}-A_{m,n}S_{m,n+2}-B_{m,n}S_{m,n+1}}{C_{m,n}} \tag{D.8}$$

The associated time and boundary conditions are (see Sec. 2.5):

$$S_{1,n>1} = -\sqrt{\left[\frac{U_{e1}}{U_{e2}}\right]}\, f_{2_{1,\sqrt{\left[\frac{U_{e1}}{U_{e2}}\right]}n}} + \left(\frac{U_{e1}}{U_{e2}} - 1\right)(n-1)H$$

$$+ f_{2_{1,n}} \tag{D.9}$$

$$\frac{\partial S_{m,100}}{\partial \eta} = 0 = \frac{1}{2\Delta\eta}\left[-3\,S_{m,100} + 4\,S_{m,99} - S_{m,98}\right] \tag{D.10}$$

$$\frac{\partial S_{m,1}}{\partial \eta} = 0 = \frac{1}{2\Delta\eta}\left[-3\,S_{m,1} + 4\,S_{m,2} - S_{m,3}\right] \tag{D.11}$$

and

$$S_{m,1} = 0 \tag{D.12}$$

First, the $S_{m,n}$ distribution was obtained for $0 \leq \tau \leq 1$ using the recurrence relations (3.1), (3.2), and (3.3). Later, equations (D.8) through (D.12) were used to modify the $S_{m,n}$ distribution to incorporate the full molecule into the calculations. However, the convergence (if any) was too slow and the method was given up.

APPENDIX 'E'

EFFECT OF THE VARIATION OF GRID SIZE

Figure E.1 shows the effect of the variation of grid size upon the value of stream function increment Δf . The elementary step sizes in the η and τ directions are denoted by H and T respectively. As we keep the value of H fixed and vary the step size T in the direction of τ , we notice that the maximum variation in the value of Δf happens to be about 5.8% when the step size T is reduced to one-tenth of its previous value of 0.05. However, the leading derivative terms in expression (2.31) indicate its parabolic nature and, therefore, it will not be proper to take excessively small steps in the τ-direction, which will lead to large round off errors [25].

For a constant value of T, the maximum variation in the value of Δf with the variation in H has been noticed to be 2.5% when H is reduced to one-half of its previous value of 0.1.

Lastly, it should be mentioned that the smaller step sizes also give rise to computer-storage problems (especially, if one wants to use double precision for calculations) and also the numerical approach becomes costly computer time-wise. Keeping in view these facts it was decided to keep step size H = 0.1 in the η-direction and step size T = 0.05 in the τ-direction.

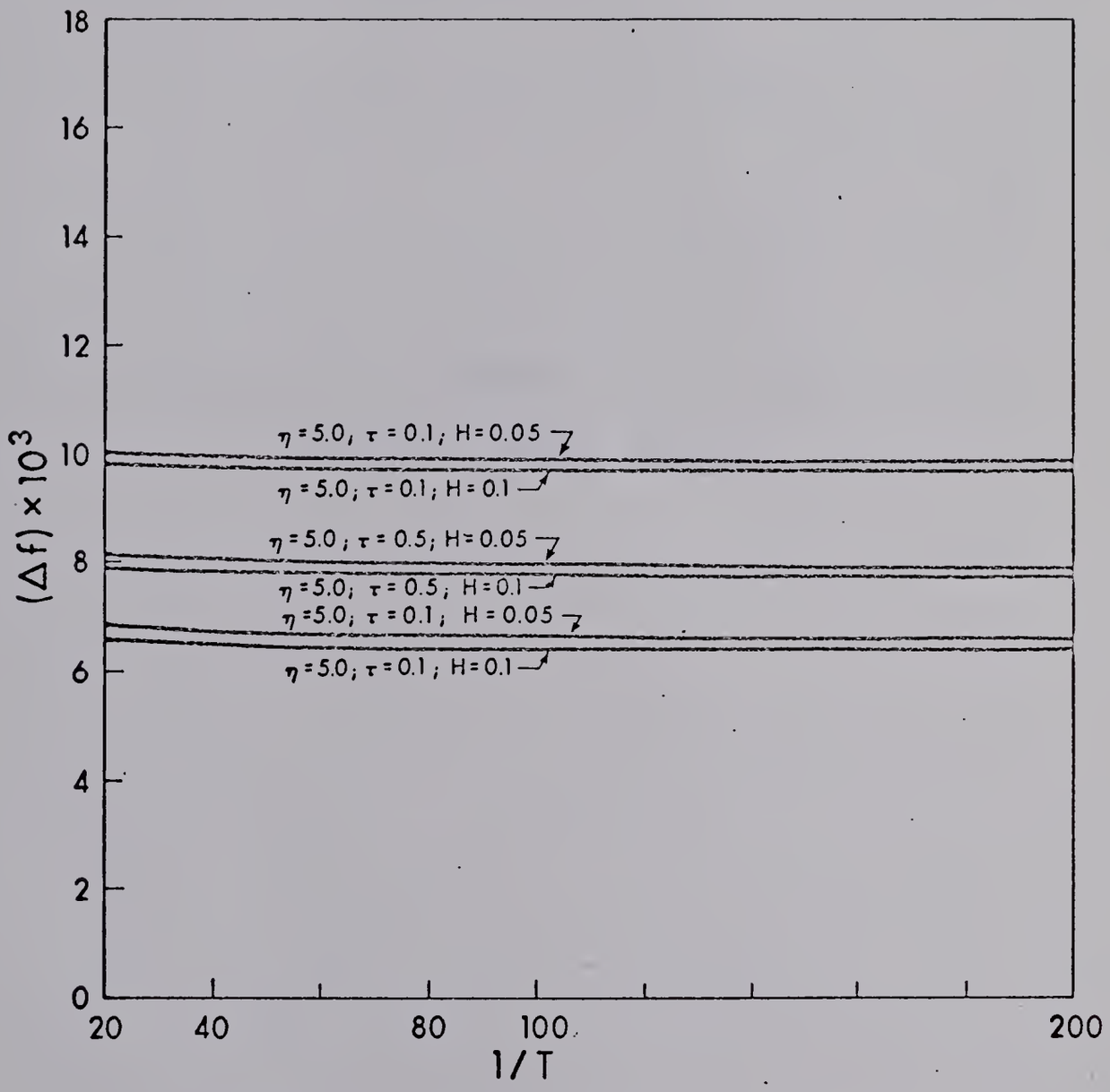

Fig. E.1 Effect of the Variation of Grid Size on the Value of Stream Function Increment Δf

APPENDIX 'F'

CURVES FOR CHAPTER III & IV

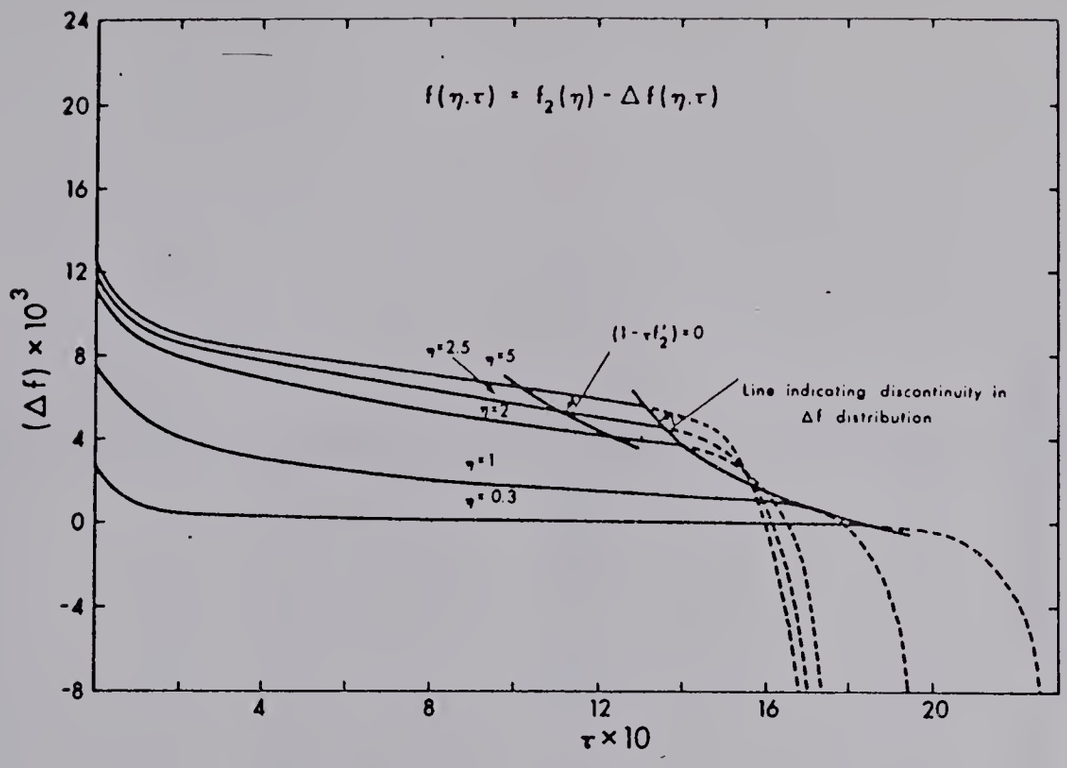

Fig. 3.3 Stream Function Increment (Δf) Distribution Curve

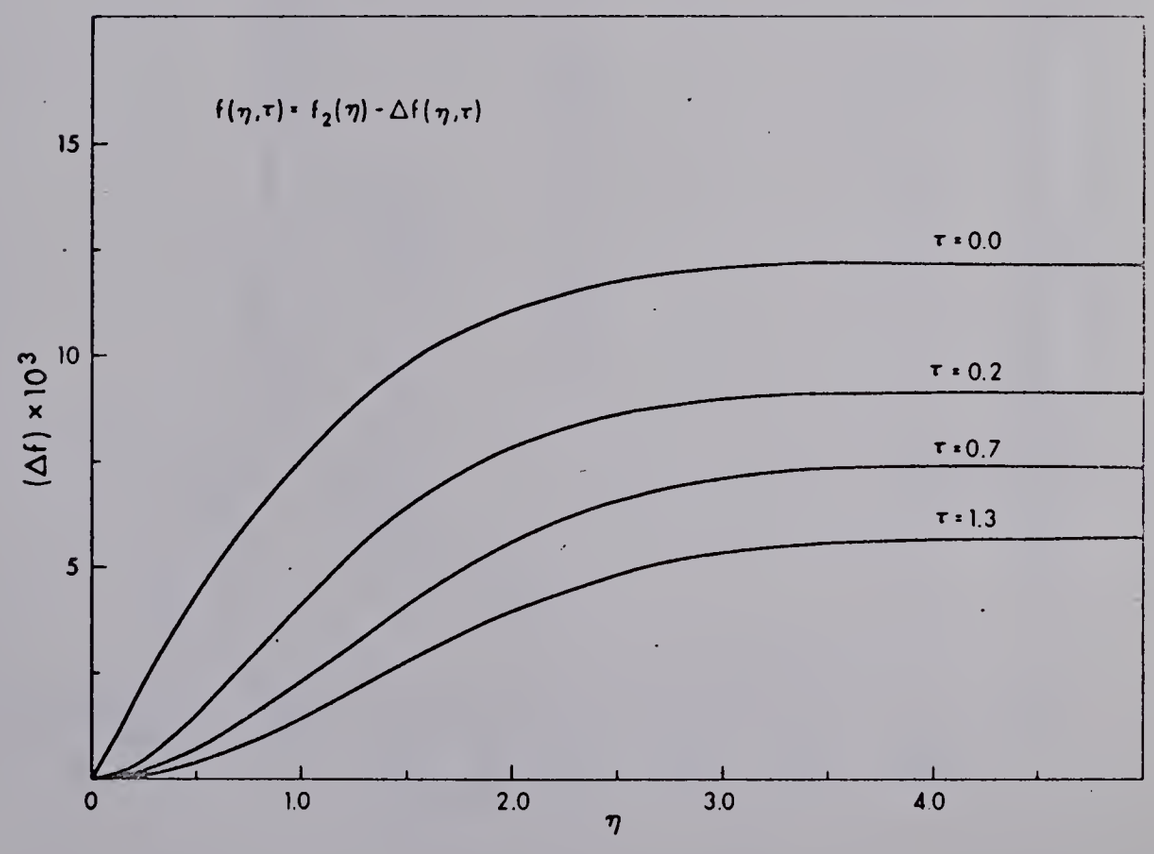

Fig. 3.4 Profiles of Stream Function Increment Δf

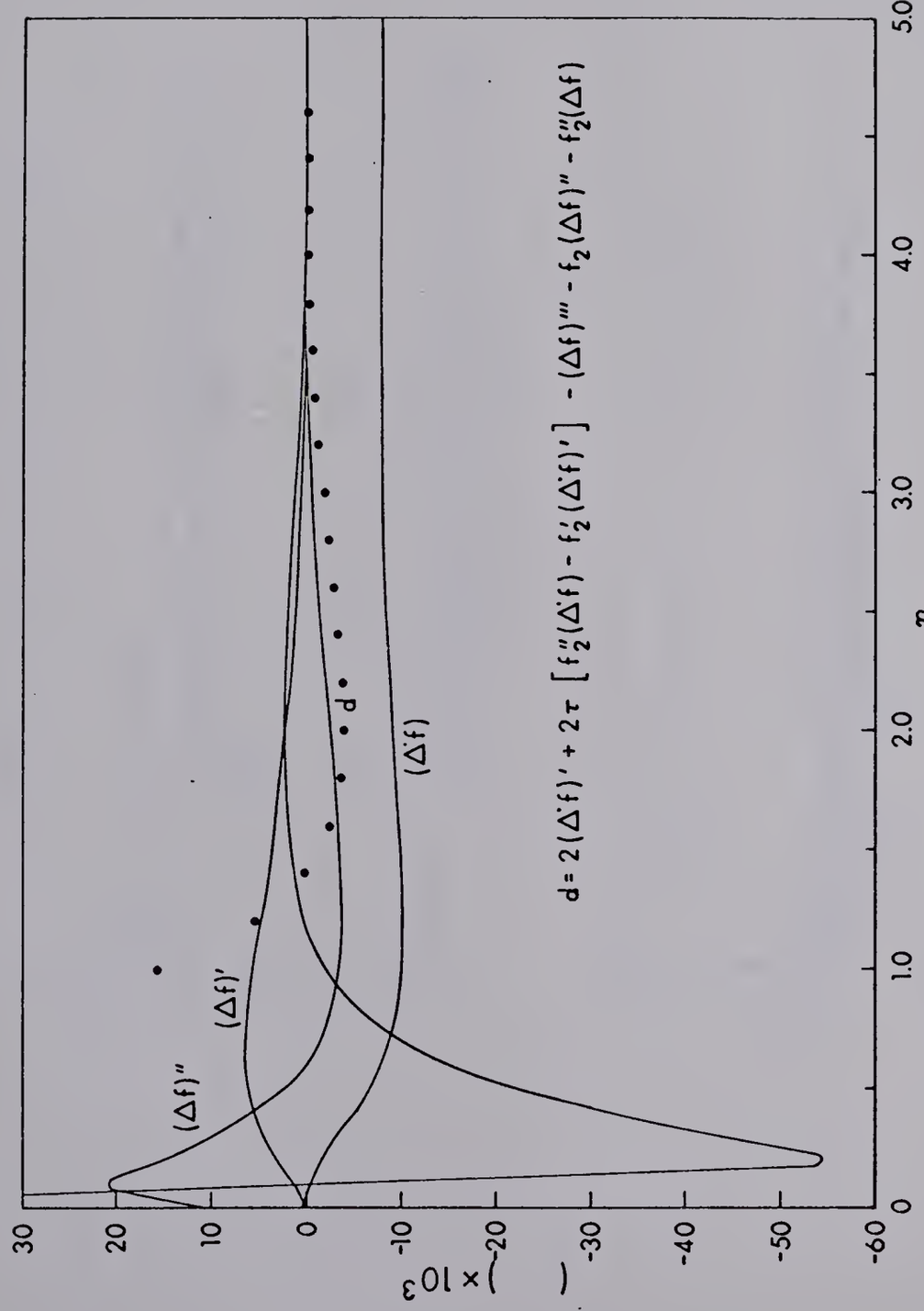

Fig. 3.5 Distribution of the Derivatives of Δf (for τ=0.1) and Verification of the Satisfaction of the Differential EQuation (...)

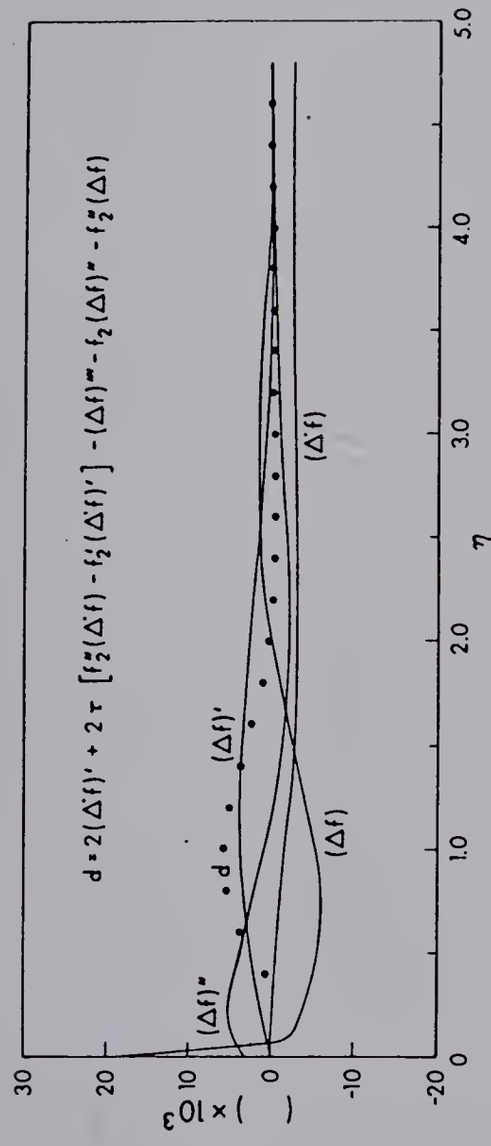

Fig. 3.6 Distribution of the Derivatives of Δf (for τ=0.7) and Verification of the Satisfaction of the Differential Equation

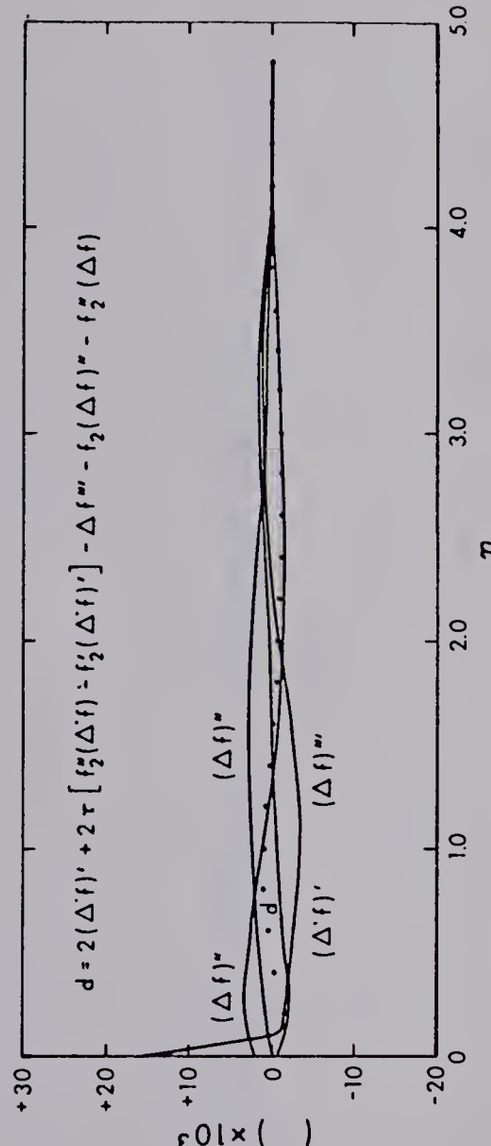

Fig. 3.7 Distribution of the Derivatives of Δf (for τ=1.3) and Veritification of the Satisfaction of the Differential Equation (...)

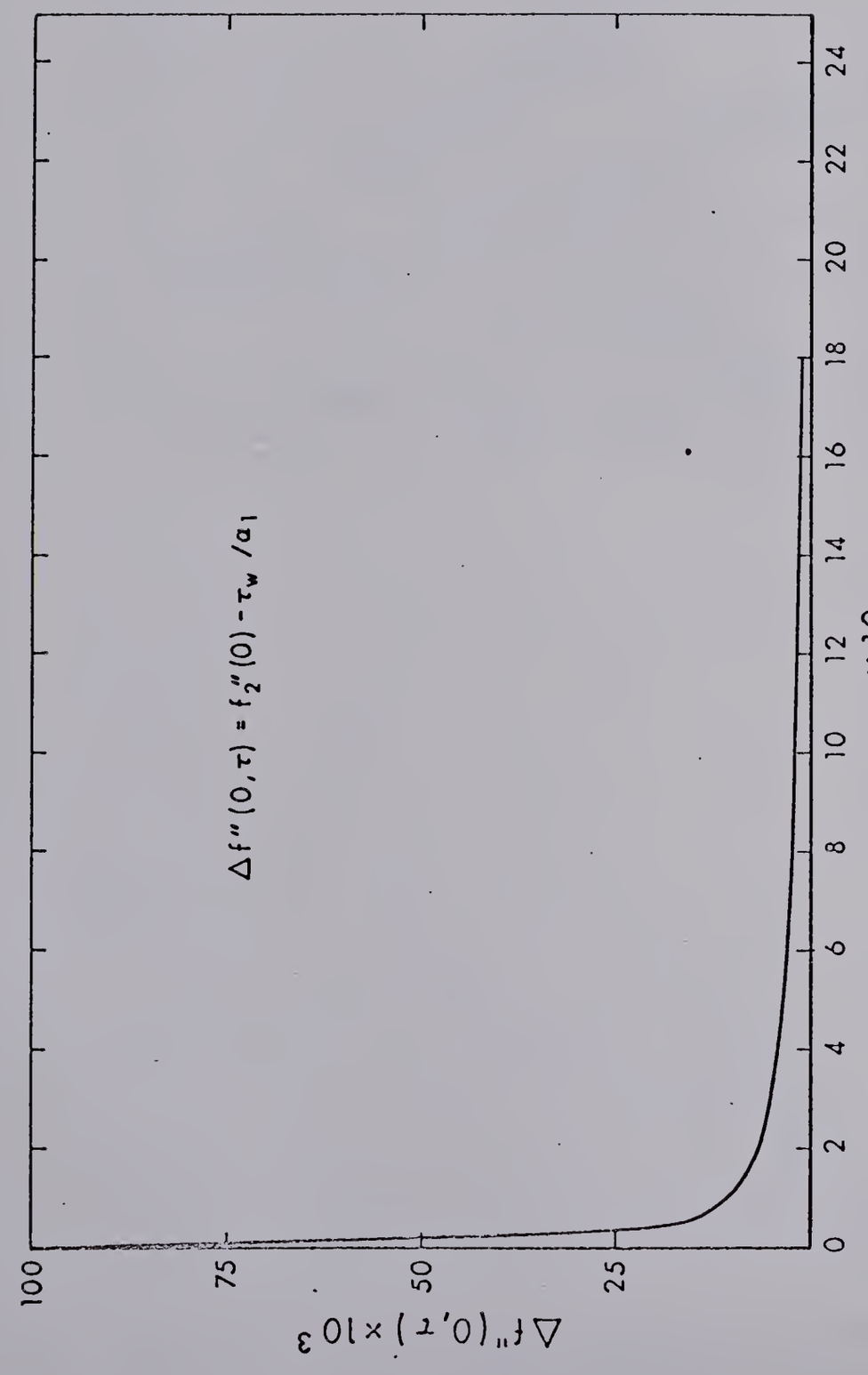

Fig. 3.8 Distribution of the Shearing Stress at the Wall

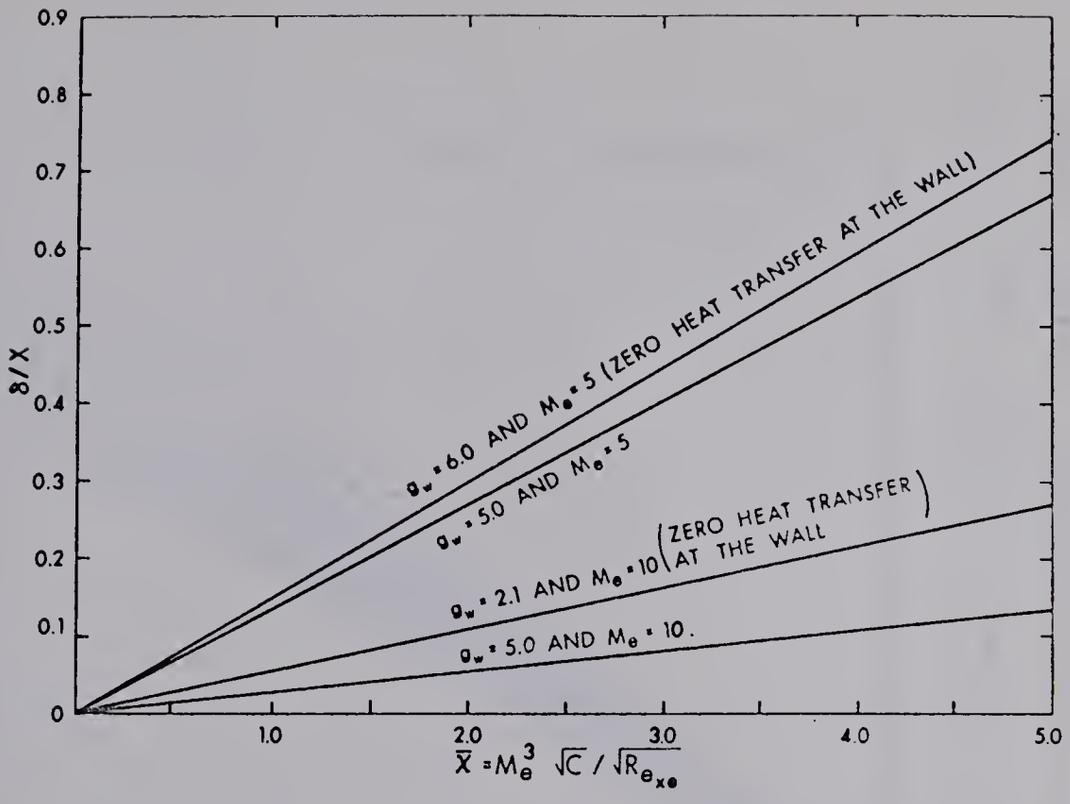

Fig. 4.1 Boundary Layer Thickness Over a Flat Plate
(Pr=1, γ=1.4)

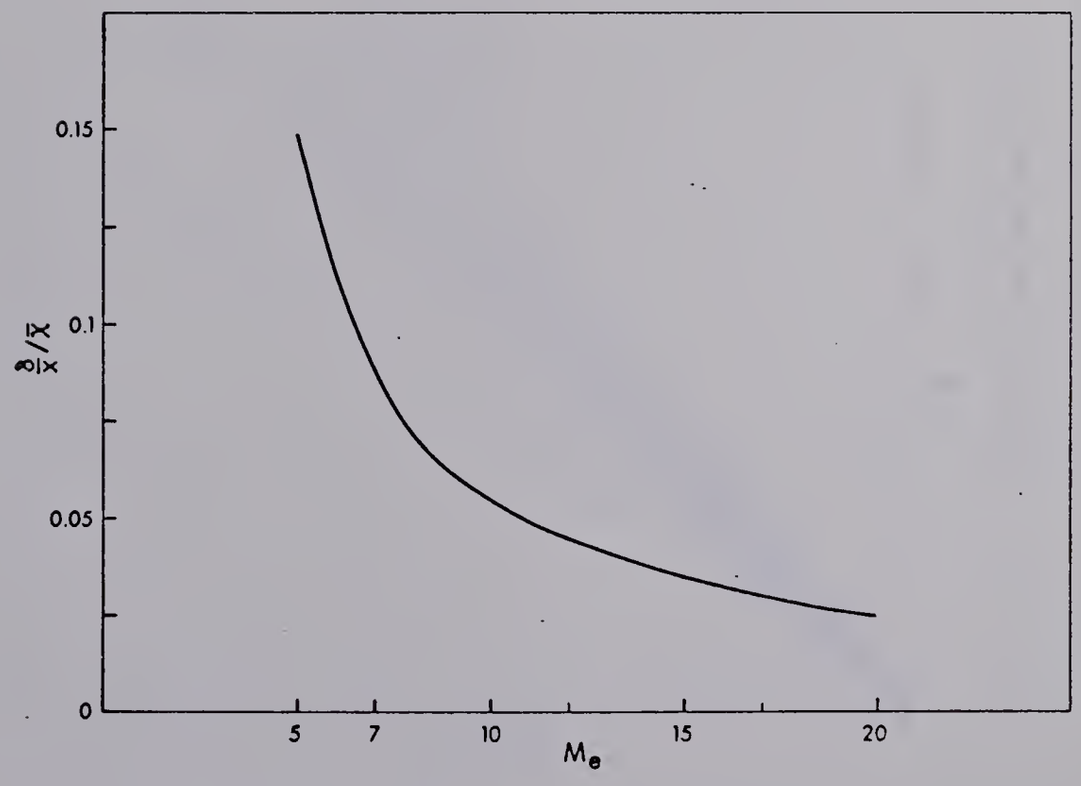

Fig. 4.2 Boundary Layer Thickness Over a Flat Plate
(Pr=1, γ=1.4)
(For zero heat transfer at the wall)

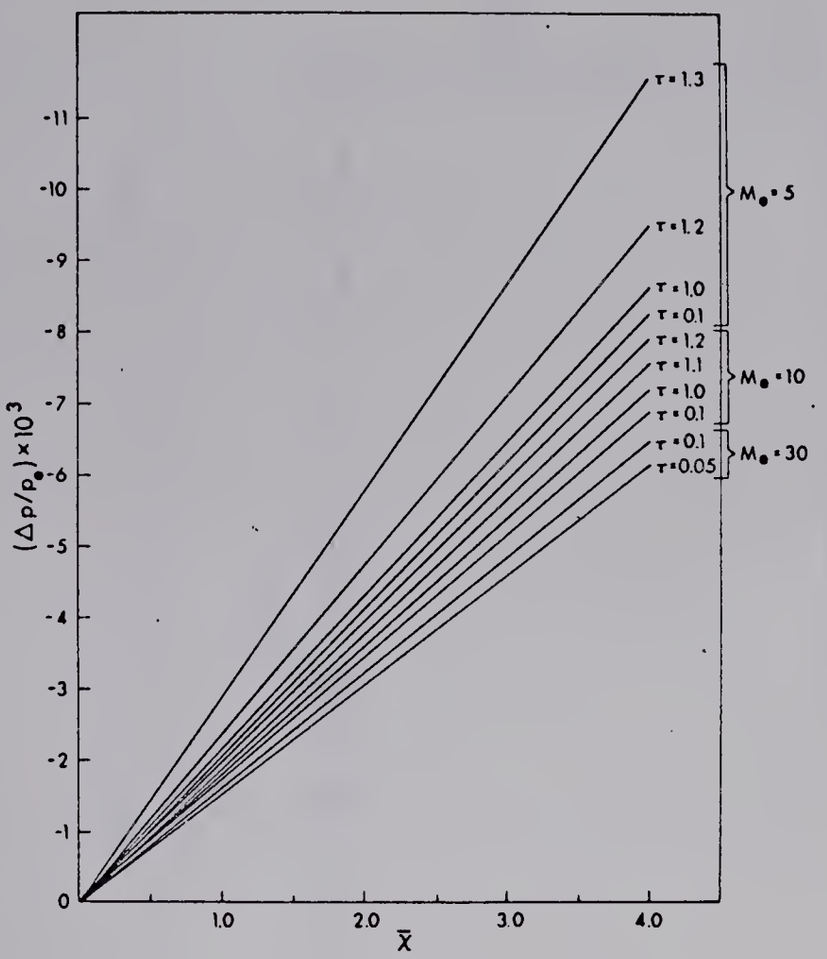

Fig. 4.3a Stepwise-decelerated flow

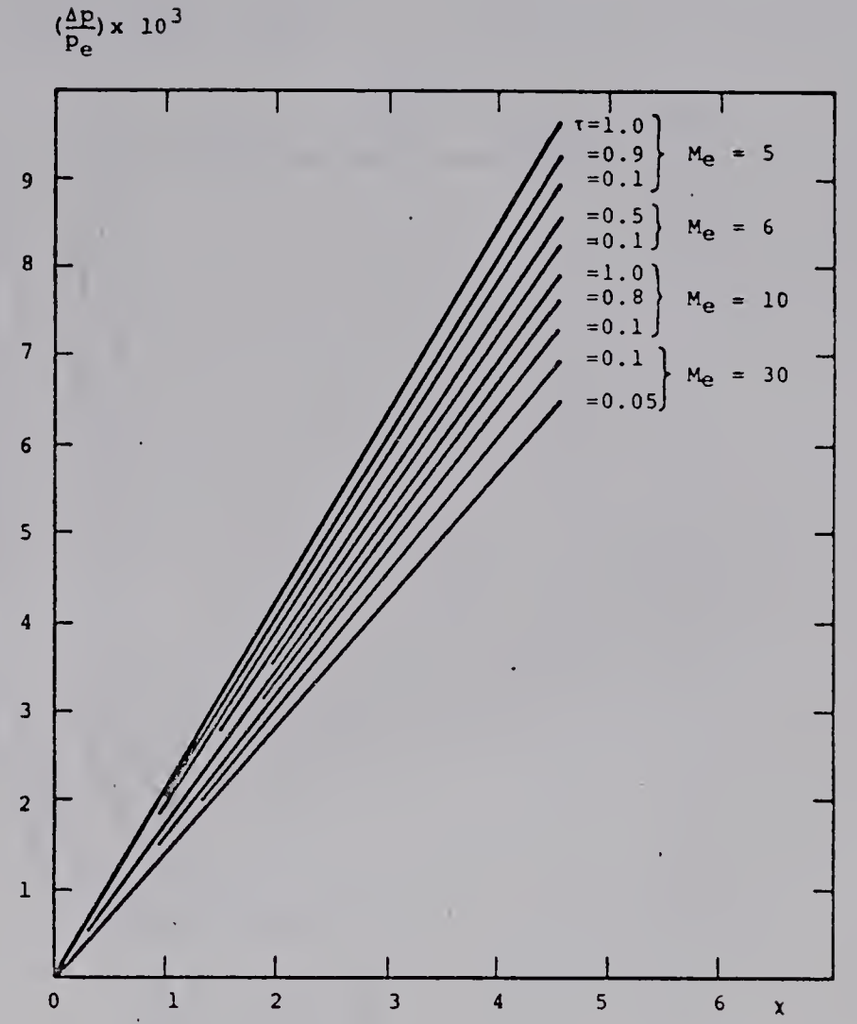

Fig. 4.3b Stepwise-accelerated flow (Ref. [3])

Transient Contribution to the Induced Pressure for the Case of No Heat Transfer at the Wall

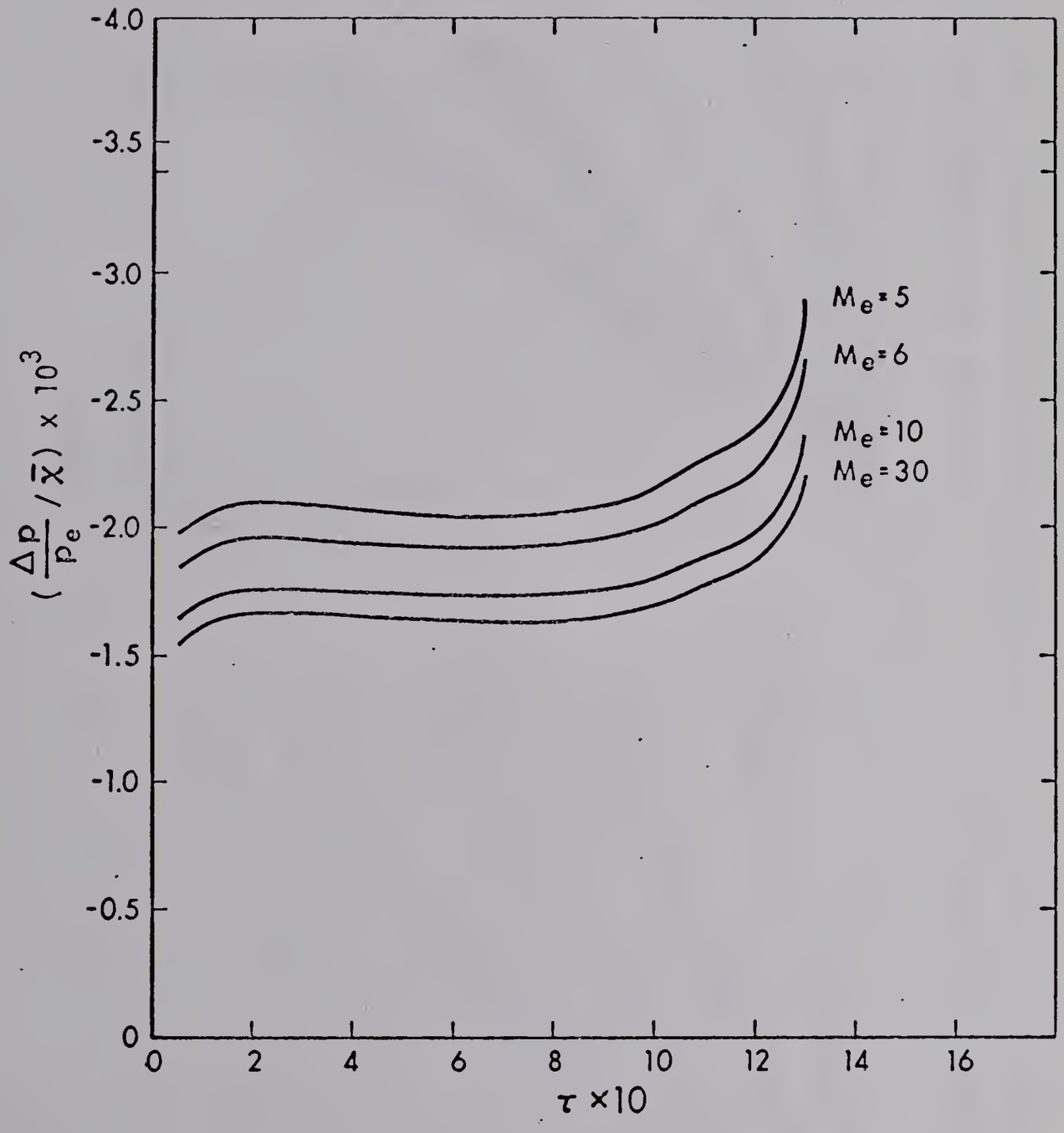

Fig. 4.3c Transient Contribution to the Induced Pressure for the Case of No Heat Transfer

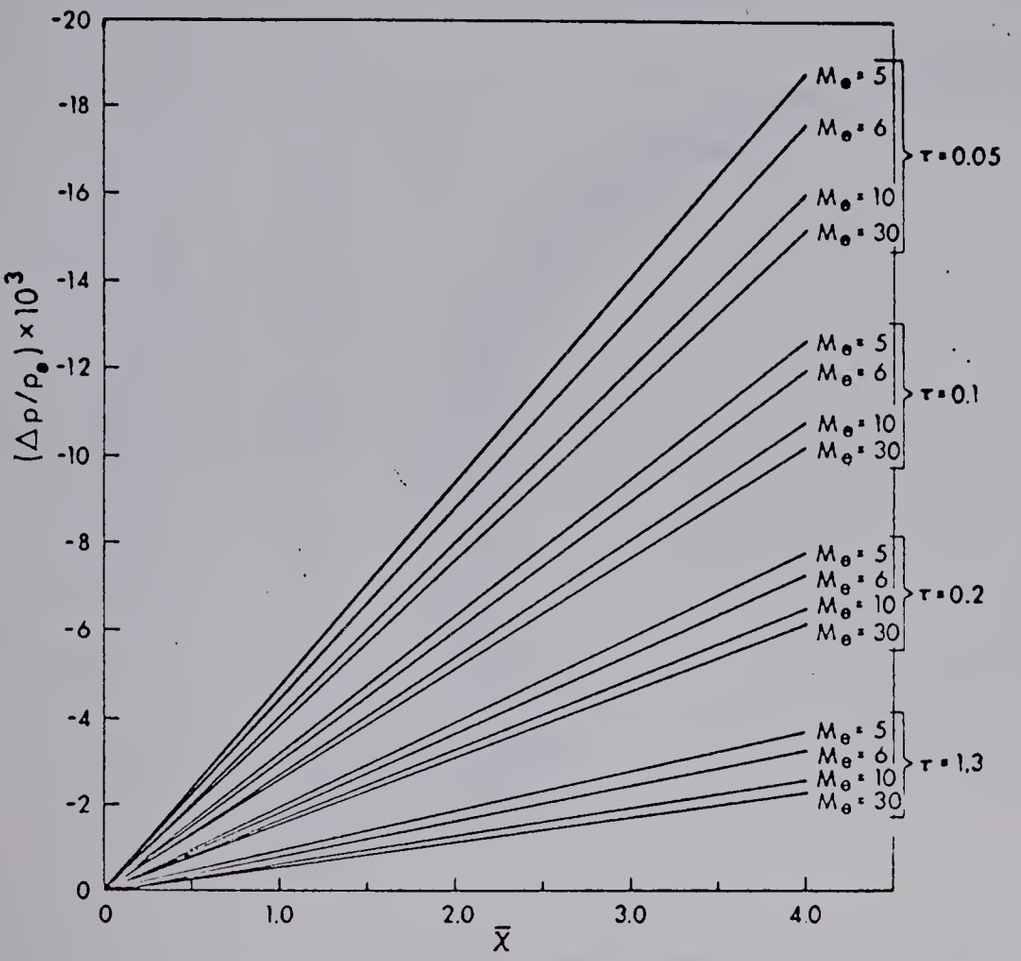

Fig. 4.4a Stepwise-decelerated flow

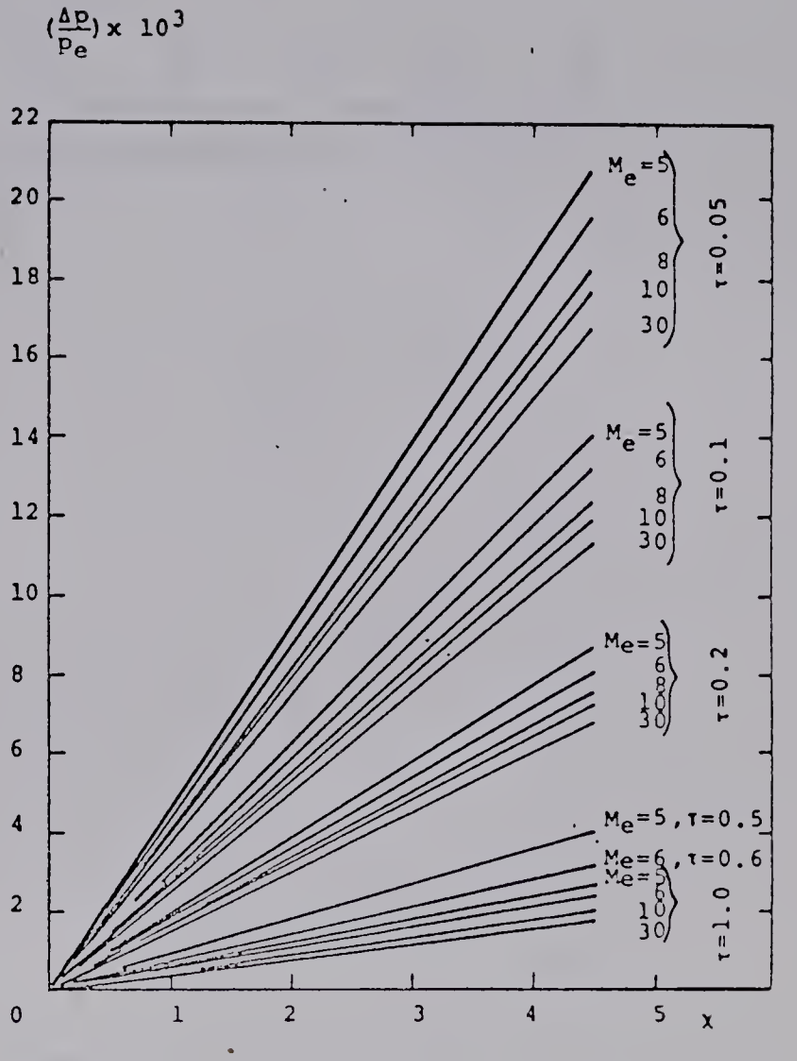

Fig. 4.4b Stepwise-accelerated flow (Ref. [3])

Transient Contribution to the Induced Pressure for the Case of $g_w = 0.0$

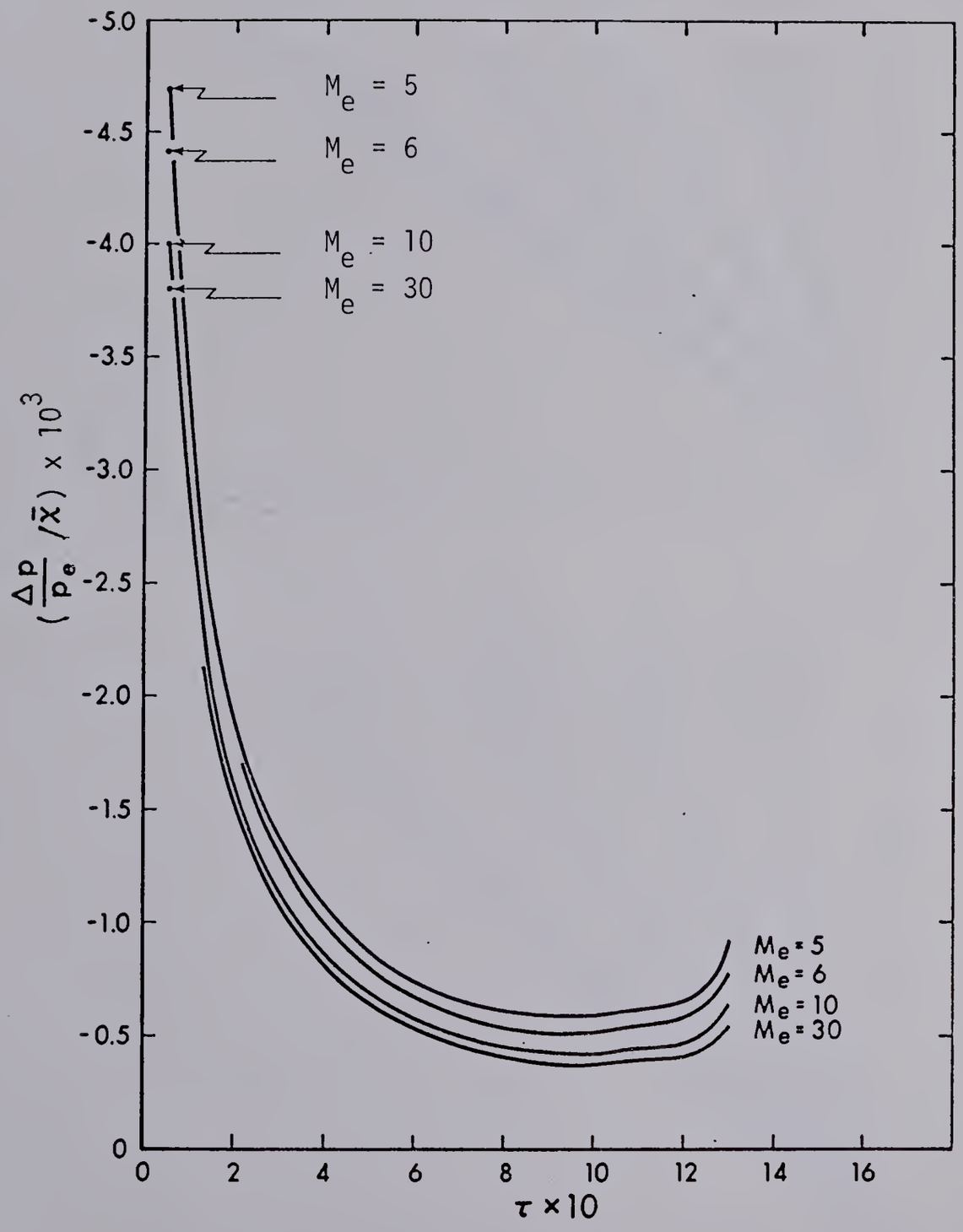

Fig. 4.4c Transient Contribution to the Induced Pressure for the Case of $g_w = 0.0$

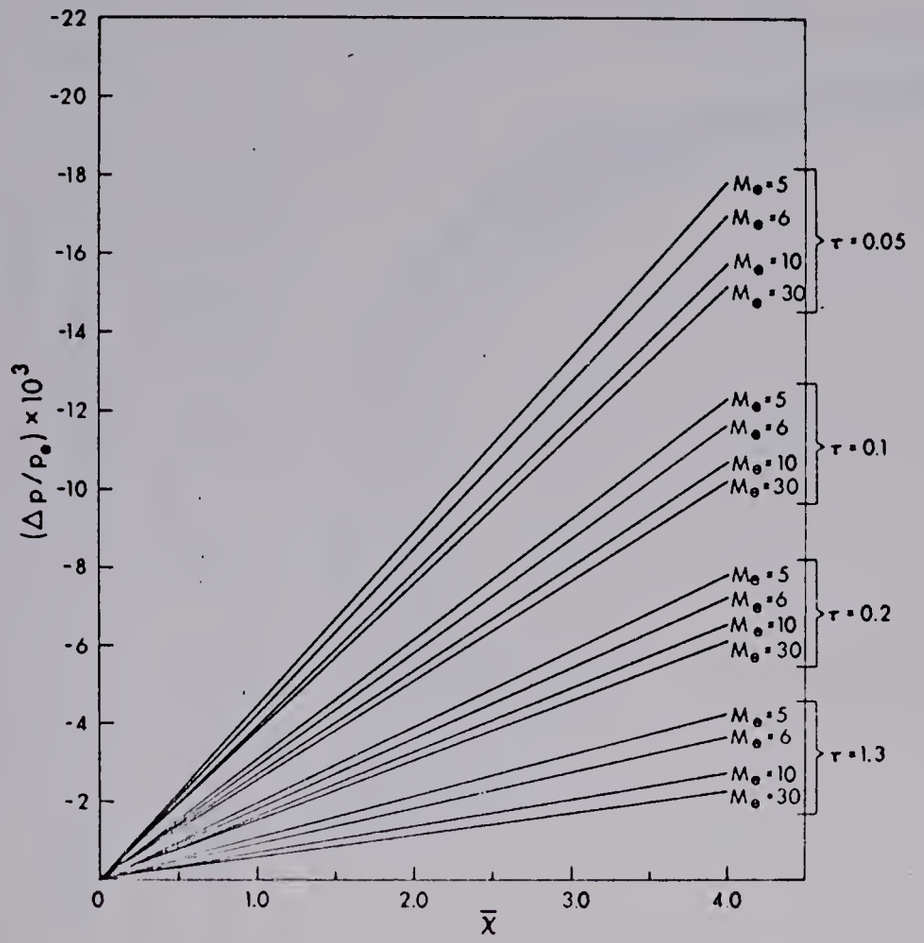

Fig. 4.5a Stepwise-decelerated flow

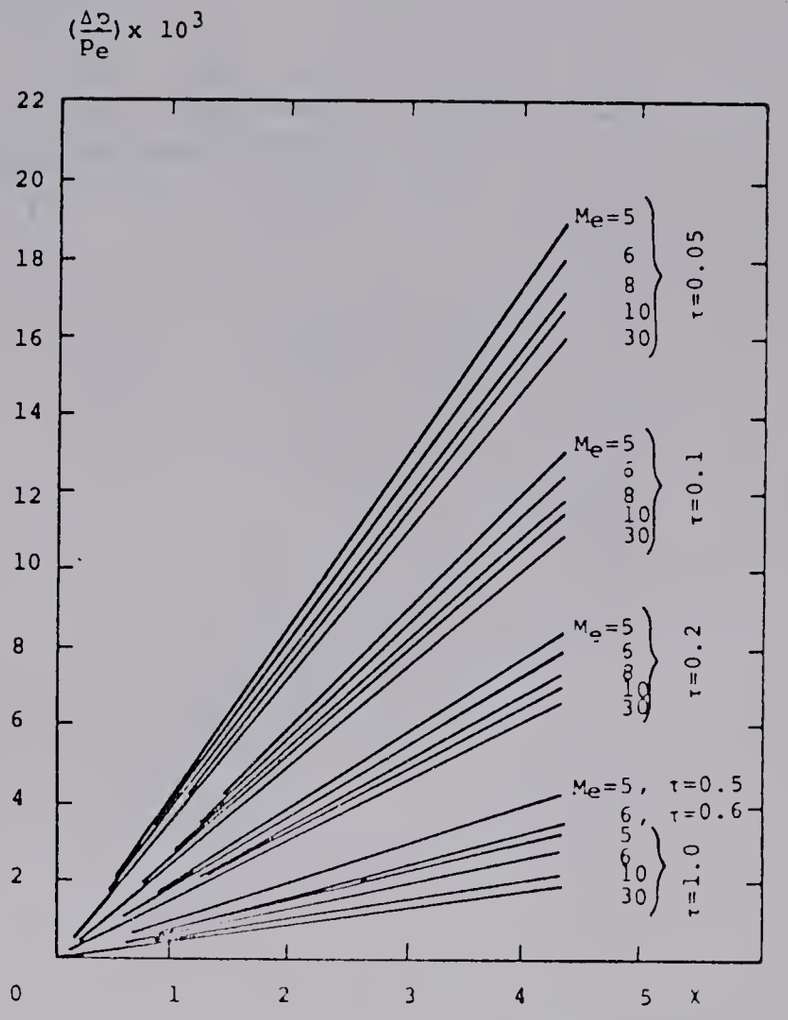

Fig. 4.5b Stepwise-accelerated flow (Ref. [3])

Transient Contribution to the Induced Pressure for the Case of $g_w = 0.5$

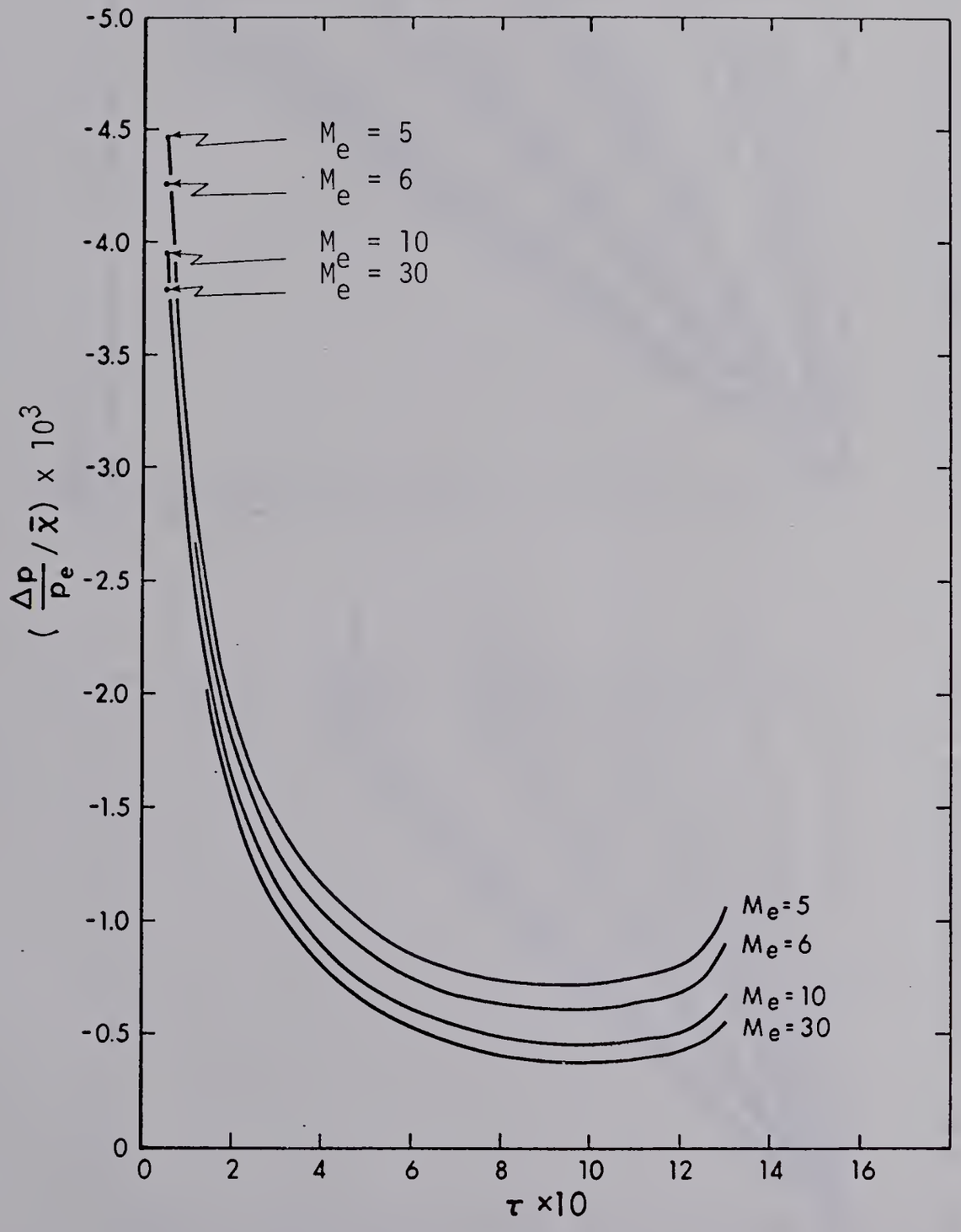

Fig. 4.5c Transient Contribution to the Induced Pressure for the Case of $g_w = 0.5$

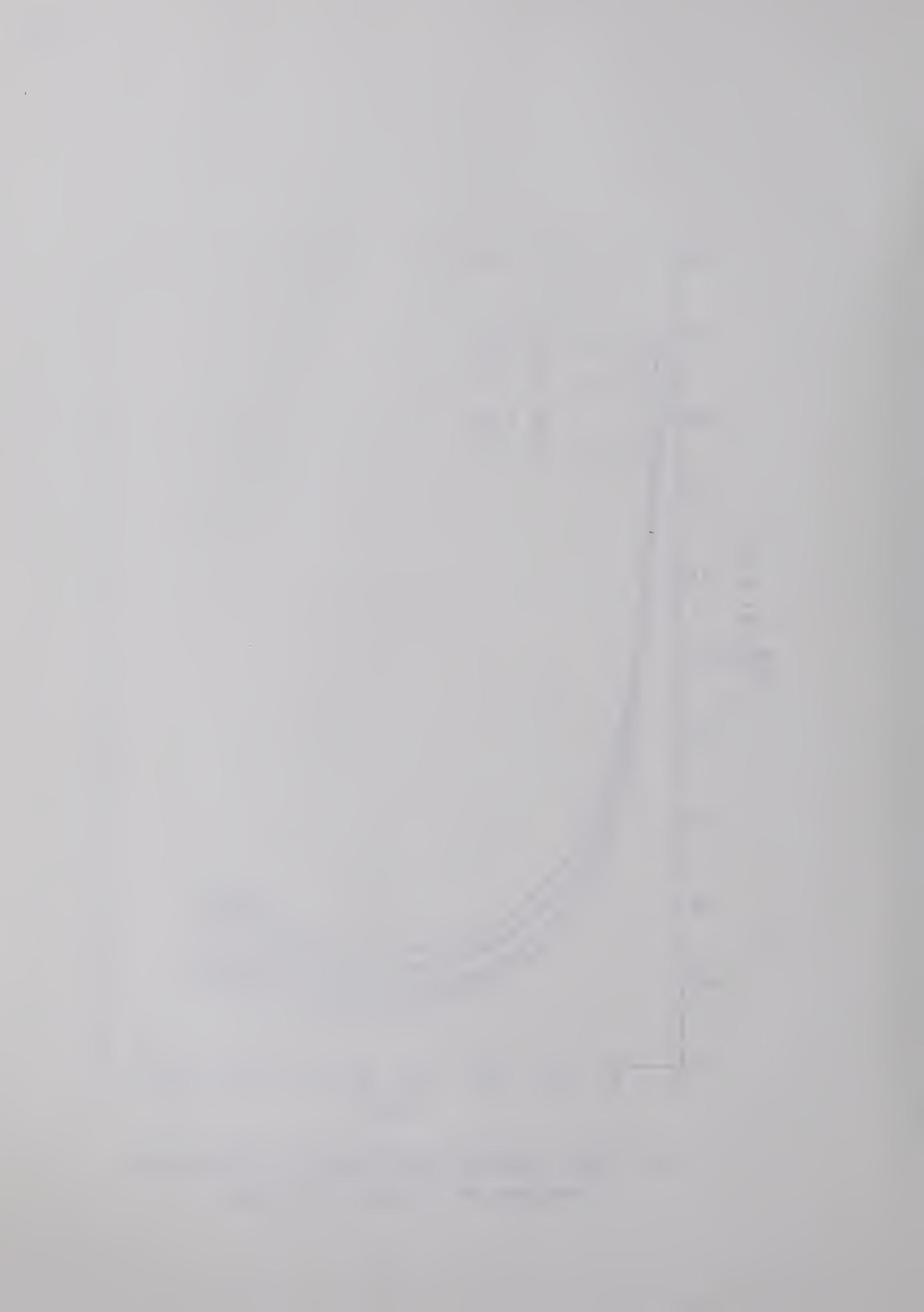

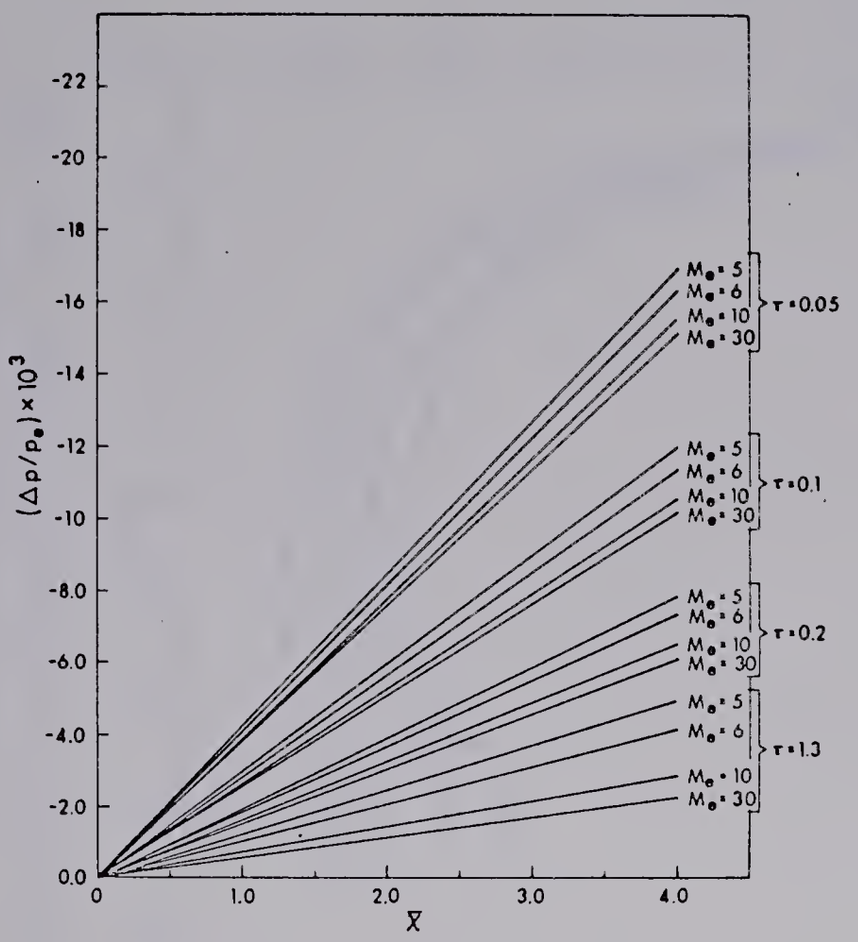

Fig. 4.6a Stepwise-decelerated flow

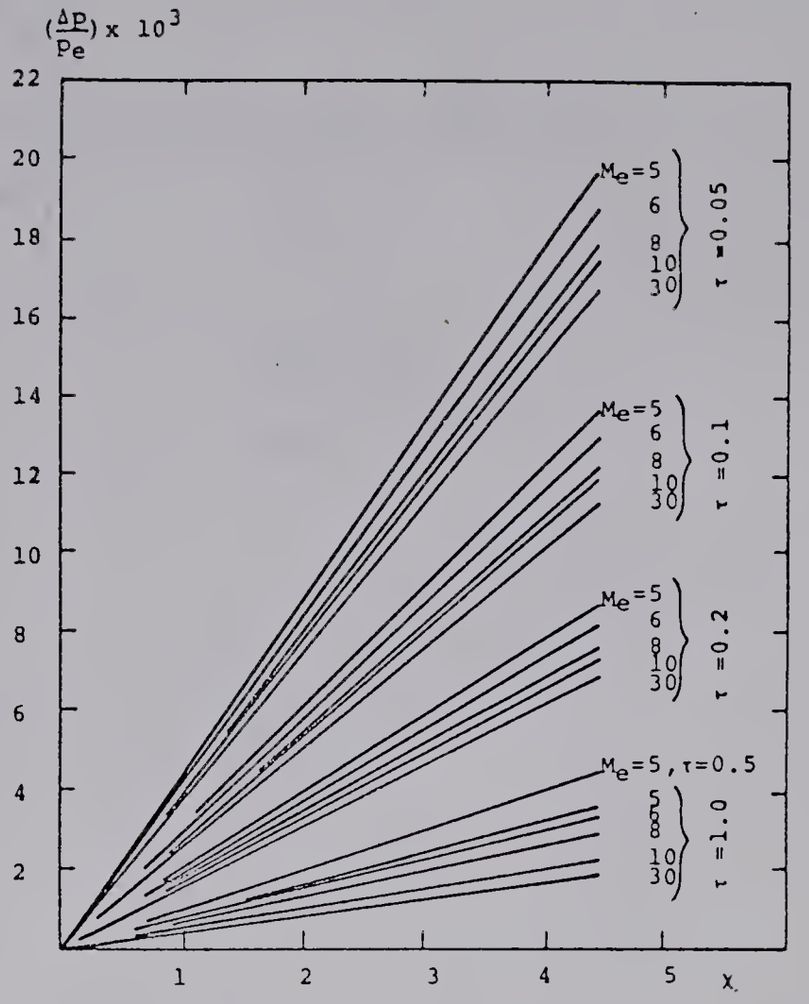

Fig. 4.6b Stepwise-accelerated flow (Ref. [3])

Transient Contribution to the Induced Pressure for the Case of g_w = 1.0

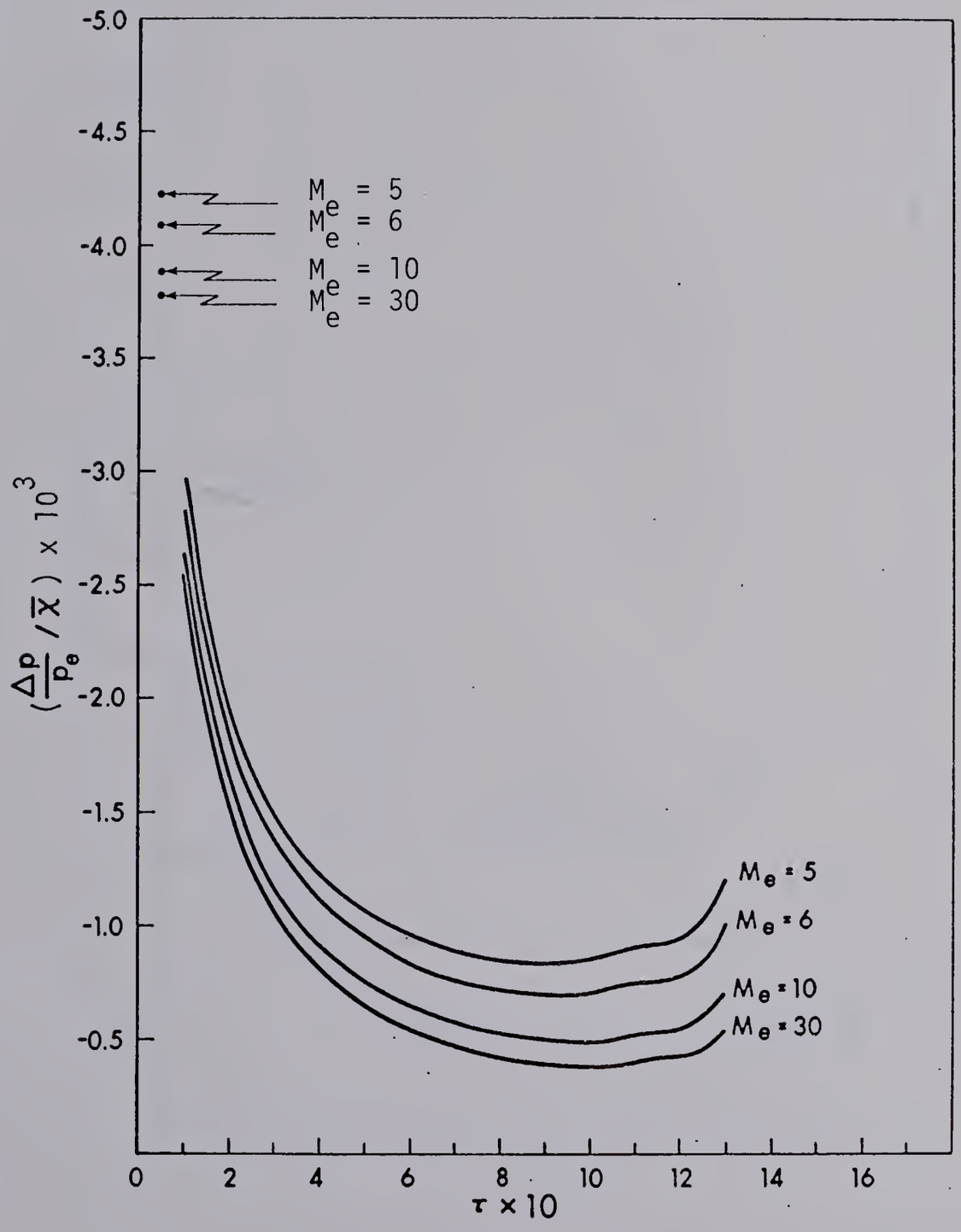

Fig. 4.6c Transient Contribution to the Induced Pressure for the Case of $g_w = 1.0$

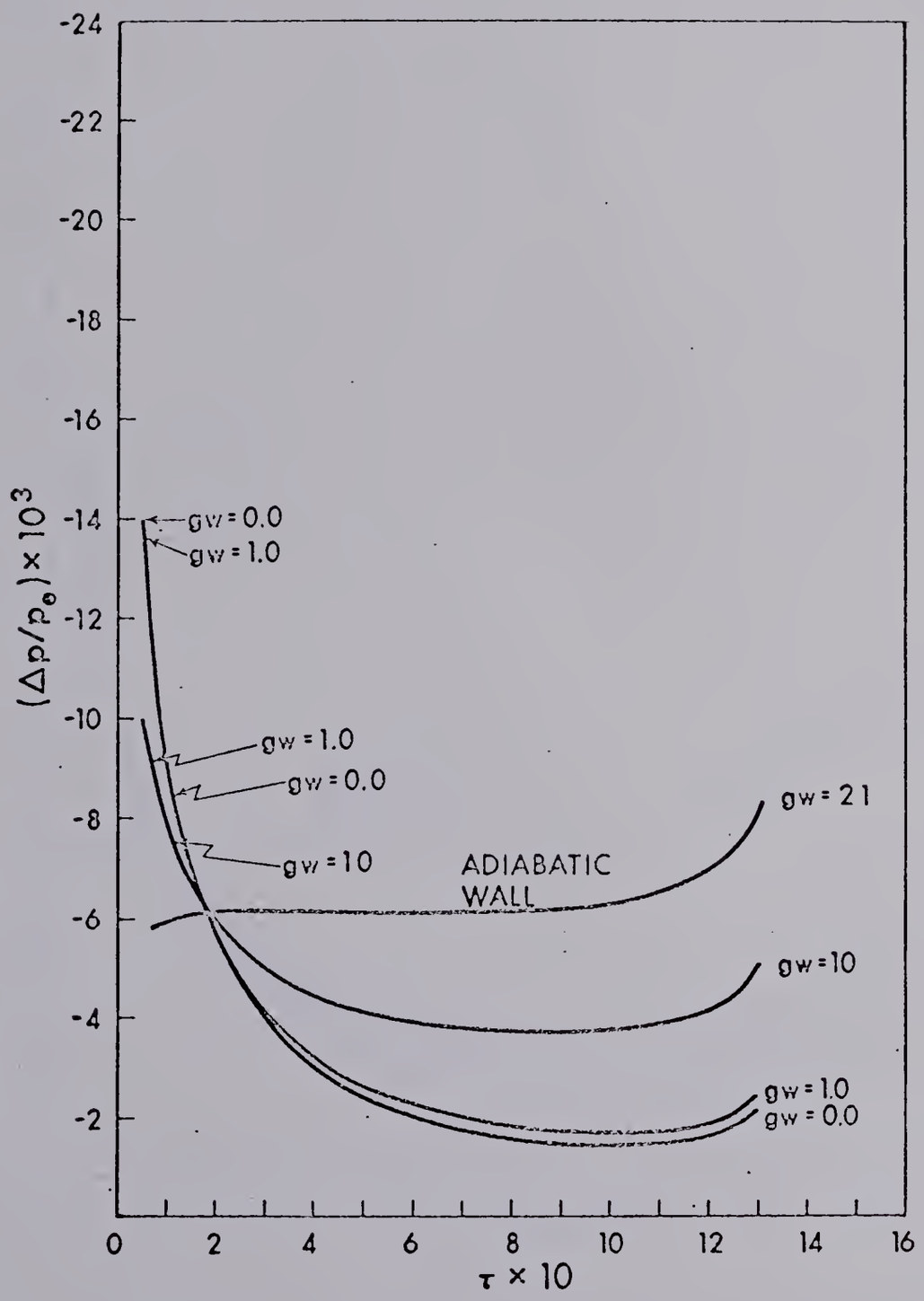

Fig. 4.7 Transient Contribution to the Induced Pressure for the case of $\overline{\chi} = 3.5$ and $M_e = 10$

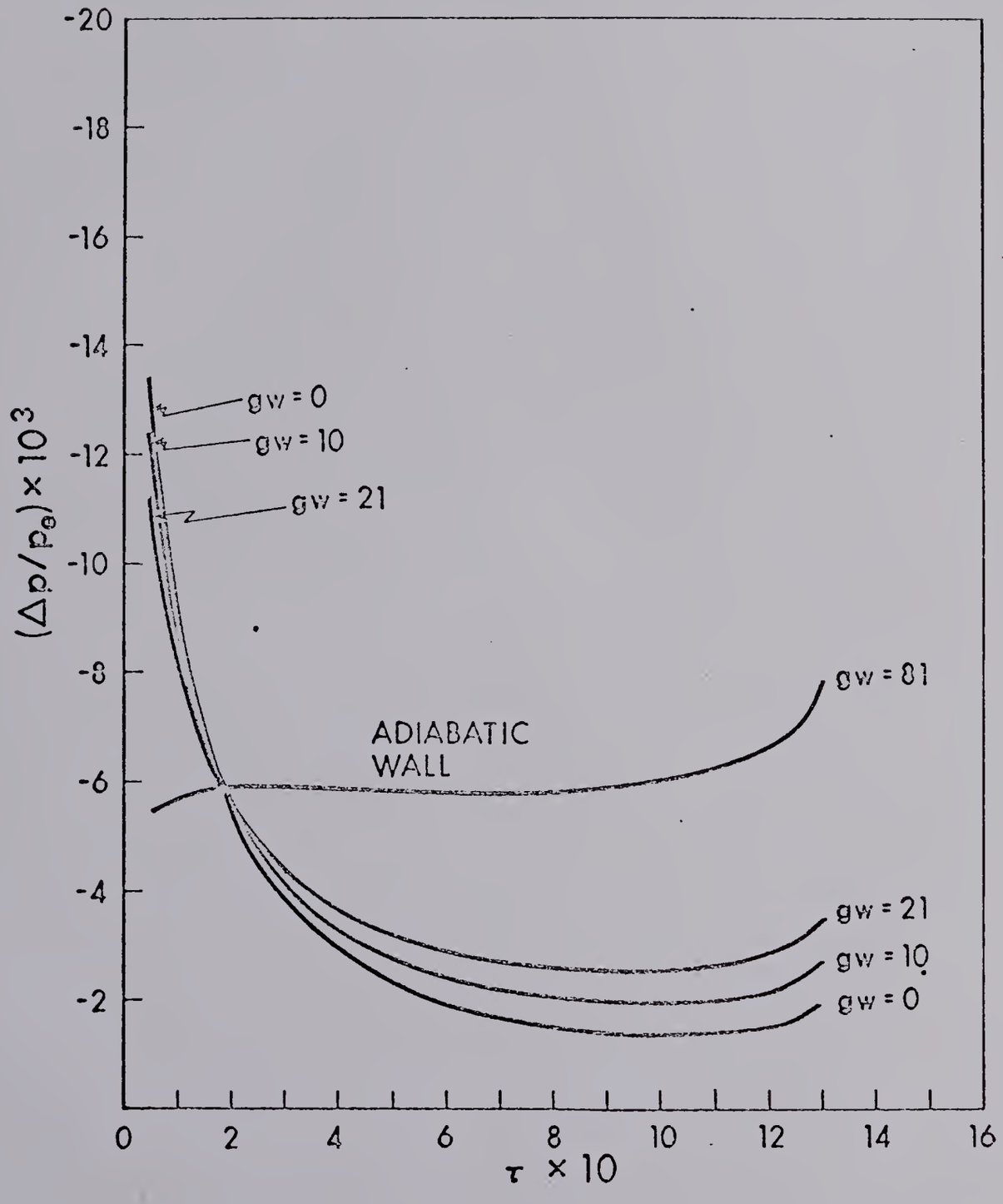

Fig. 4.8 Transient Contribution to the Induced Pressure for the Case of $\bar{\chi} = 3.5$ and $M_e = 20$

B29882